DOI: 10.1070/RCR4797

Towards rational design of metal-organic framework-based drug delivery systems

Anna A. Simagina,[a] Mikhail V. Polynski,[a] Alexander V. Vinogradov,[a] Evgeny A. Pidko [a, b]

[a] *Saint Petersburg National Research University of Information Technologies, Mechanics and Optics (ITMO University)*
ul. Lomonosova 9, 191002 Saint Petersburg, Russian Federation
[b] *Delft University of Technology*
Van der Maasweg 9, 2629 HZ Delft, the Netherlands

Metal-organic frameworks comprise a class of crystalline porous coordination polymers with unique chemical and physical properties. On the one hand, due to high specific surface area, biocompatibility and stability in biological media, framework materials are ideal candidates for the development of new dosage forms, in particular, for drug delivery systems. On the other hand, the modular structure of frameworks provides an opportunity for computational screening and predictive calculations. This opens new prospects for the design of modern functional materials. The computational screening and simulation of adsorption – desorption processes play a key role in the development of drug delivery systems, as they provide data that are difficult to obtain solely from experiments. These data can greatly assist in the development of drug delivery systems. The first part of the review gives a brief overview of the metal-organic frameworks which have already proved to be potential drug carriers as well as frameworks which are currently being extensively studied and gain attention in this area. The second part addresses the concept of rational design and computer-aided design of such systems.
The bibliography includes 216 references.

Contents

1. Introduction 831
2. Metal-organic frameworks 833
3. Computer simulation for the rational design of MOF-based materials for targeted drug delivery 842
4. Conclusion 853

1. Introduction

Framework materials, or frameworks (metal-organic and covalent organic frameworks) are a rapidly developing family of hybrid porous compounds applicable for a variety of purposes including gas storage,[1, 2] optics[3] and catalysis.[4]

First of all, let us clarify the terminology: in the literature, the term 'coordination polymers' may sometimes rufer to mean framework materials; most often, this concerns metal-organic frameworks. In this review, we adhere

A.A.Simagina. Engineer at ITMO University.
E-mail: simagina@scamt-itmo.ru
Current research interests: metal-organic frameworks, covalent organic frameworks, computer simulation of framework materials, computer simulation of adsorption, pharmaceutical chemistry.
M.V.Polynski. Engineer at ITMO University.
E-mail: polynski@scamt-itmo.ru
Current research interests: modelling of catalytic processes, *ab initio* molecular dynamics, modelling of multicomponent systems, automation of quantum chemical studies.
A.V.Vinogradov. Candidate of Chemical Sciences, Associate Professor, Chief Researcher, Director of the Biochemistry Cluster of ITMO University.
E-mail: avv@scamt-itmo.ru
Current research interests: inorganic chemistry, metal-organic frameworks, ink-jet printing, sol – gel chemistry, non-linear optical effects.
E.A.Pidko. Ph.D. in Chemistry, Professor, Chief Researcher at ITMO University, Associate Professor, Chair at Delft University of Technology (the Netherlands).
Telephone: +31(15)278 – 1938, e-mail: pidko@scamt-itmo.ru
Current research interests: inorganic chemistry, computational chemistry, modelling of catalytic processes, density functional theory, determination of reaction mechanisms.

Received 11 November 2017
Translation: Z.P.Svitanko

© 2018 Uspekhi Khimii, Russian Academy of Sciences and Turpion Ltd.

to the terminology accepted at the expert IUPAC meeting [5] held in 2013, according to which coordination polymer is 'a coordination compound with repeating coordination entities extending in 1, 2 or 3 dimensions'. Coordination network is 'a coordination compound extending, through repeating coordination entities, in 1 dimension, but with cross-links between two or more individual chains, loops or spiro-links, or a coordination compound extending through repeating coordination entities in 2 or 3 dimensions'. Metal-organic framework (MOF) is a coordination network with organic ligands containing numerous pores.[6]

Currently, there are two key methods for loading active ingredients (AIs) into the framework materials, differing by the stage in which this operation is performed: direct addition of the therapeutic agent (TA) during the synthesis and post-synthetic methods.[7]

In the former case, therapeutic agents are incorporated into the framework pores during the synthesis *via* encapsulation or doping. The key feature of the direct loading is that AIs are added during the synthesis as dopants in order to impart materials with additional functions, with the obtained particles preserving the properties and morphology of the initial materials. During the direct loading, molecules are encapsulated in the pores, mainly, as a result of covalent interactions. This method has been used to encapsulate a number of agents for the subsequent application of the resulting framework-based hybrid materials as chromophores, chemotherapeutic agents, drug delivery systems, *etc*. The preparation of MOFs with biologically active components (bioMOFs) can also be attributed to this group.

The second group of methods comprises post-synthetic modification of MOFs. First, the framework material is synthesized and activated. Then the active ingredient is loaded *via* sorption, most often, from a solution. This method inolves non-covalent binding of guest molecules (Fig. 1 *a*). The development of MOF-based drug delivery systems provides good results regarding both drug loading into MOFs and drug release. For example, an ibuprofen storage capacity of 1.4 g g^{-1} has been achieved,[8] as well as prolonged and stable release from the cavities without premature degradation of the material. Post-synthetic covalent modification giving rise to a prodrug attached to the framework material has been reported (Fig. 1 *b*),[9] with drug release being due to material degradation.[10] Co-crystallization has also become a popular method for post-synthetic loading of TAs into framework pores.[11]

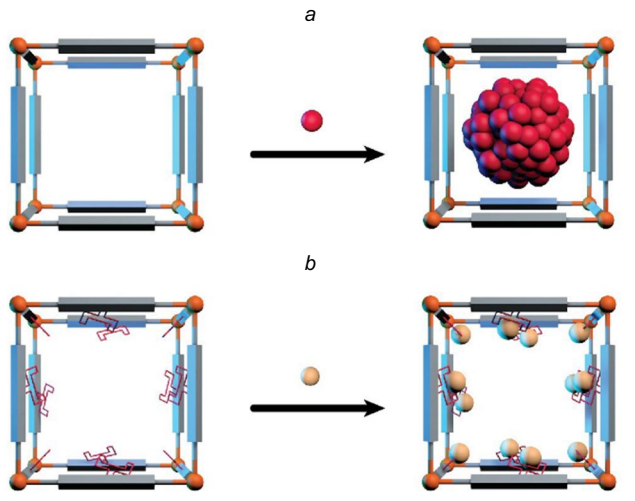


Figure 1. Scheme reflecting non-covalent (*a*) and covalent (*b*) ways of loading active ingredients into framework materials. The model metal-organic framework is depicted as a cage and the model therapeutic agent is shown as spheres.

The following abbreviations are used in the review:

AI — active ingredient;

API — active pharmaceutical ingredient

bioMOF — metal-organic framework containing biologically active molecules

IRMOF — iso-reticular metal-organic framework

COF — covalent organic framework

TA — therapeutic agent

siRNA — small interfering RNA

MOF — metal-organic framework

NMOF — nano metal-organic framework

AASBU — automated assembly of secondary building units

AmAc — amino acid

AmD — amphiphilic dendrimer

AuToGraFS — automated topological generator for framework structures

B97 — Becke exchange-correlation functional

BDC — benzene-1,4-dicarboxylic acid

B3LYP — Becke, 3-parameter, Lee-Yang-Parr functional

BTC — benzene-1,3,5-tricatboxylic acid

BTW-FF — Bristow–Tiana–Walsh force field

CADD — computer-aided drug design

CD — cyclodextrin

CNTs — carbon nanotubes

CP correction — counterpoise correction for basis set superposition error

CS — chitosan

CSD — Cambridge Structural Database

CuJAST — $[Cu_2(BDC)_2(ted)]_n$ (ted is triethylenediamine)

CYCU — Chung Yuan Christian University MOFs

def-SV(P) — Alrichs split valence double-ζ polarized basis set

def2-TZVP — Alrichs split valence triple-ζ polarized basis set

DFT — density functional theory

DMA — dimethylammonium cation

DNP — double-ζ polarization function basis set

DWES — Dubbeldam–Walton–Ellis–Snurr force field

ESP — electrostatic potential methods

FA — folic acid

FACS — folic acid conjugated chitosan

5-FAM — 5-carboxyfluorescein

FITZ-HSA — canine endothelial sarcoma cell line

5-FU — 5-fluorouracil

6-311**G — Gaussian type orbital basis set

GGA — generalized gradient approximations

HA — hyaluronic acid

HeLa — human cervical carcinoma cell line

HKUST — Hong Kong University of Science and Technology materials

HL60 — human acute myeloid leukaemia cells;

HMSN — hollow mesoporous silica nanoparticles

HRP — horseradish peroxidase;

HT-29 — human colon adenocarcinoma cells
IBU — ibuprofen
ipa — isophthalic acid
LANL2DZ — Los Alamos National Laboratory basis set of double zeta quality
MBP — metal-binding protein
MD — molecular dynamics
MIL — materials of Institut Lavoisier
MP — Møller – Plesset perturbation theory
MPF — metal peptide framework
MSN — mesoporous silica
MCF-7 — human breast cancer cell line
MCM-41 — a sort of mesoporous silica (mobil composition of matter No. 41)
mtz — 5-methyltetrazole
MW — microwave radiation
MWCNTs — multi-walled carbon nanotubes
NCI-H292 — non-small cell lung cancer cell line
NIH/3T3 — murine fibroblast cells
PAA — polyacrylic acid
PAMAM — polyamidoamine
PBS — phosphate-buffered saline
PBE — Perdew – Burke – Ernzerhof exchange correlation functional
PBEsol — modified exchange correlation PBE functional
PCN — porous coordination network
PD/MNMOF — photodynamic magnetic NMOF
PEG — polyethylene glycol
Periodic DFT — density functional theory calculations in periodic boundary conditions
PW91 — Perdew–Wang exchange correlation functional
PAW — projector augmented wave method
pcS-n — pseudocontact chemical shift basis set
Phen — phenanthroline
PMNP — polymeric magnetic nanoparticles
QD — quantum dot
QSAR — quantitative structure – activity relationships
REF52WT — rat embryonic fibroblasts
RI — resolution of identity
SBA-15 — a sort of mesoporous silica
SBU — secondary building unit
SCS — spin-component scaling
thb — tetrahydrobiopterin
tpta — 5,5′-(pyridine-2,5-diyl)diisophthalate anion
TTI-COF — triazine triphenyl imine-based covalent organic framework
UFF — universal force field;
USPIO — ultrasmall superparamagnetic iron oxide
vdW-DF — non-local exchange-correlation functional
ver — verapamil
VV10 — Vydrov–Van Voorhis non-local exchange-correlation functional
ZIF — zeolite imidazolate frameworks

2. Metal-organic frameworks

Although metal-organic frameworks were classified as a separate type of chemical compounds only in the early 21st century, quite a few publications addressing MOF-based drug delivery systems have already appeared, demonstrating the efficiency of both sorption of drug molecules in the framework cavities [12] and drug release.[13]

The combination of crystallinity, unique porous structure, high specific surface area and mechanical flexibility favourably distinguishes this class among other materials. The combination of metal ions and organic ligands gives freedom to control both structural and physical (*e.g.*, magnetic) properties, while high sensitivity to external conditions gives an additional option for the control of material characteristics.[2]

2.1. Structural features of metal-organic frameworks

While classifying and integrating the knowledge on MOF structures, O'Keeffe and Yaghi [14] developed a system based on network topology analysis. According to their classification, the inorganic and organic components are considered as secondary building units (SBU), from which it is possible to fabricate the whole structure (Fig. 2).

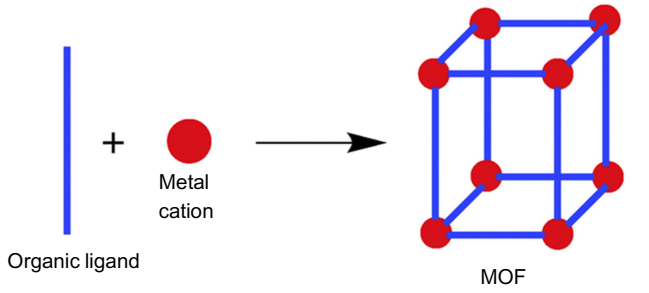


Figure 2. Basic diagram of the structure of metal-organic frameworks.

The identification and description of the networks providing understanding of the key MOF topologies resulted in a database of these networks and opened up a way for the rational structure design. From the practical standpoint, this knowledge is of crucial importance for the control over MOF synthesis and parameterization of the synthesis *via* modular process, which is called reticular synthesis.

Furthermore, by varying the basic units that compose MOFs, it is possible to fabricate complex multilevel materials with unique properties. The structural complexity of MOFs can be compared with the structure of proteins and described using a similar four-level hierarchy:[15, 16, 17]

— primary structure: organic ligands, metal cations and the coordination sphere. This is the first structural level comprising the key framework units such as building blocks or secondary building units;

— secondary structure: the specific assembly of the building blocks for the formation of crystal structure, which may give rise to different network topologies;

— tertiary structure: interaction between the linkers and the formation of interlaced networks. This structural level is associated with important effects such as structure dynamics and flexibility. It can be considered the first supramolecular level;

— quaternary structure: this level refers to a possible interaction with other structural units such as the framework – guest interactions. It can be regarded as the second supramolecular level.

Due to the considerable interest in MOFs as drug delivery systems, a large body of data on various MOF-based containers has now been accumulated and needs to be classified. Most popular is the classification system developed for porous polymers by Kitagawa and Kondo,[18] which can be adapted to MOFs.[19] In the classical version, all framework materials are subdivided into three generations. First generation compounds disintegrate as the guests are removed. Second generation materials have a strong rigid structure and retain crystallinity when no guests are in the pores. Third generation materials are transformable and can undergo structural modifications.

This classification has been further developed in a recent review [20] dealing with biomedical applications of MOFs, in which a more detailed interpretation of the three MOF generations is presented.

(1) First generation (Fig. 3 *a*): parameters of the starting material (surface area and pore volume) are employed for encapsulation of active molecules, which should be subsequently released in the target cells, while the early material degradation before the target is reached should be avoided. Furthermore, this first generation includes materials composed of simple biomolecules and biocompatible metal cations (bioMOFs).

(2) Second generation (Fig. 3 *b*): surface modification to increase the biocompatibility of MOFs and to attain targeted delivery (nMOFs). Second generation frameworks are expected to overcome the existing restrictions on the controlled drug release. This class comprises MOFs that are relatively tolerant to guest molecules (can contain an adsorbate within the cavities for a long period of time without considerable destruction of the crystal structure and also survive the drug release).

(3) Third generation (Fig. 3 *c*): development of multifunctional and biocompatible drug delivery systems with targeted action by means of special signals and contrast agents.

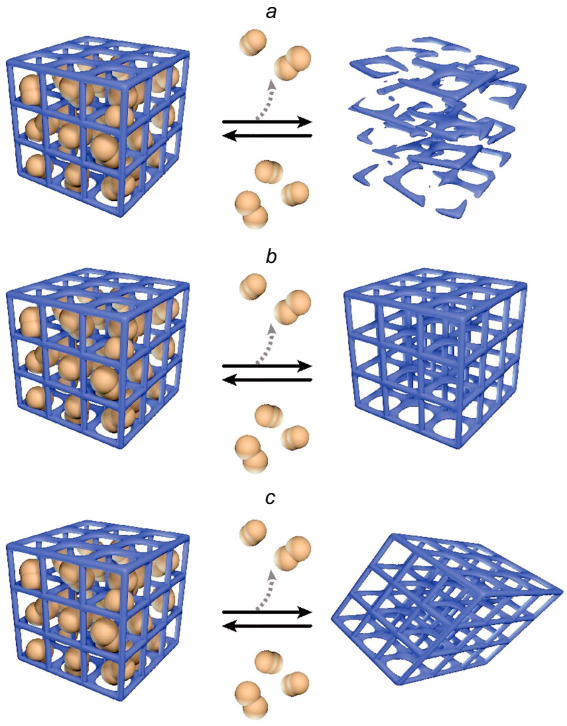


Figure 3. Model representation of three generations of metal-organic frameworks according to Kitagawa classification.[19]
The model metal-organic framework is depicted as a cage and the model therapeutic agent is shown as spheres.

2.2. Metal-organic framework containers for drug delivery systems

The metal-organic frameworks are proposed more and more often as drug delivery containers owing to their properties such as well-defined highly porous structures, switchability of the inner surface nature from hydrophobic to hydrophilic, the ability to incorporate functional groups, use of biorelevant metals and/or bioactive linkers as well as the controlled stability of materials.

Since the appearance of MOFs and until now, the most popular MOFs for drug delivery considered in the greatest number of publications are those developed by a research team at the Lavoisier Institute, which are, therefore, called materials of Institut Lavoisier (MIL).[21] In the most widely used structures suitable for TA loading, such as MIL-100 and MIL-101, the coordination unit comprises a trivalent metal atom (Al, Cr or Fe) and di- or tricarboxylic acids (BDC and BTC) as bridging ligands (Table 1). The MIL group of frameworks is characterized by a large surface area ($3100-5900\ m^2\ g^{-1}$) [23] and pore volume (the diameter varies in the 25 – 34 Å range). These properties render MIL perfect candidate containers for drug delivery.

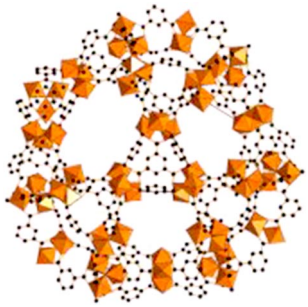
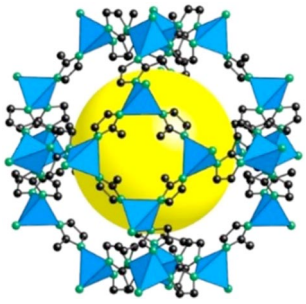
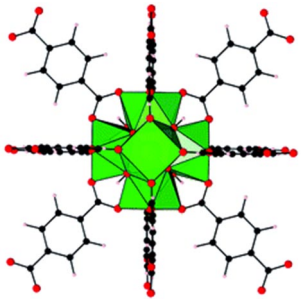
Zeolite-like imidazolate frameworks (ZIFs) represent a family of metal-organic frameworks consisting of imidazolate linkers and metal sites with tetrahedral coordination (Zn, Co, Cd, Li, *etc.*) [24] and combine broad structural variability with the possibility of formation of functionalized imidazolate linkers (see Table 1). Therefore, ZIFs form one of the largest families of MOFs known to date with more than 100 different topologies synthesized experimentally and some other topologies predicted by computer simulation.

Finally, the UIO materials [25, 26] developed at the University of Oslo and named after it form the third popular group of frameworks (see Table 1). The best known MOF of this family, UIO-66, consists of the $Zr_6O_4(OH)_4$ octahedra, which are connected to neighbouring octahedra by the benzene-1,4-dicarboxylate (BDC) linkers; this gives rise to a structure with high stability provided by the Zr – O bonds between the cluster and the carboxylate ligands.

All of the MOFs listed above have passed biocompatibility and stability tests.[27] In addition, these structures are often used as components of complex composite materials.

Unlike other well-known nano-sized porous materials such as zeolites and carbon nanotubes, in the case of MOFs, the material architecture can be controlled and the framework can be functionalized directly during the synthesis. Besides, a considerable advantage is the possibility to choose the desired components, size, shape, and chemical properties of the material by using various building blocks. Owing to the broad choice of metal sites and organic linkers, it is possible to synthesize virtually infinite number of structures with specified physicochemical properties. For example, since the MOF synthesis is temperature-dependent, the change in the synthesis temperature makes it possible to control the geometry of the inorganic component of MOFs. In addition, the MOF skeleton can consist of virtually any

Table 1. Most popular metal-organic framework families used as drug delivery containers.

Family	MIL	ZIF	UIO
	 MIL-100(Fe,Cr)	 ZIF-8-Zn($C_4N_2H_5$)$_2$	 UIO-66
Metal	Fe, Cr, Al	Zn	Zr, Hf
Ligand	Carboxylate	Imidazolate	Benzenedicarboxylate
Most popular structures	MIL-53, 88, 100, 101	ZIF-7, 8, 90	UIO-66, 67
Advantages	Considerable increase in the release time	Stability at pH 7.4 and decomposition in acid medium [22]	High stability of materials; popular compounds for the design of theranostic materials

cations, whereas zeolites, most structurally similar hybrid materials, usually contain only Al and Zn. For example, unlike mesoporous silica, MOF has a regular porous structure, which ensures reproducibility of drug loading and release; this can also be controlled by varying the composition of MOF nanoparticles (if they are formed in the synthesis).

An important challenge in the field is related to the selectivity of action of anticancer drugs, as they not only act on the damaged sites in the body, but also have a toxic effect on healthy tissues. For example, 5-fluorouracil (5-FU), which is a pyrimidine derivative, prevents nucleoside metabolism and can be erroneously incorporated in the body RNA and DNA, which induces toxic damage and apoptosis of both cancer and normal cells. In addition, there are some other shortcomings of this drug, including unstable oral availability (with variable absorption in the gastrointestinal tract and fast degradation), short elimination half-life from the plasma and development of drug resistance.[28 – 30] One more illustrative example is doxorubicin (DOX), an efficient chemotherapeutic drug against lymphoma, the application of which is also restricted by numerous adverse effects such as short biological lifetime and acute cardiotoxicity caused by its nonspecific biodistribution.[31] Therefore, these compounds are perfect candidates for the use in drug delivery systems, as this approach improves the bioavailability of such drugs, prevents untimely *in vivo* decomposition and decreases the adverse effects of drug administration

Using 5-FU and DOX, we will compare the efficiency of MOFs with other widely employed containers (Table 2). First, MOF-based delivery systems allow prolonged action of the drug without the burst effect. It can be seen in Table 2 that the general trend is to provide pH-controlled drug release. This is due to the fact that the pH level in the malignant tumour cells is below normal. Using MOF-based delivery systems, one can attain this type of drug release. Indeed, 5-fluorouracil incorporated in Fe-MIL-53-NH_2-FA-5-FAM is released faster in acid medium [32] than in a medium with pH 7.4. A considerable difference between the drug release rates at different pH has been vividly demonstrated for a P@ZIF-8-based DOX delivery system (the release in acid medium is $\sim$5 times faster).[44] As noted above, the ZIF frameworks are stable at pH 7.4, while in acid medium, they are hydrolyzed, which accounts for the popularity of these materials for the design of drug delivery systems with pH-dependent release. The efficiency of drug loading is, in this case, comparable with that for other carriers. In the case of systems containing MIL frameworks, steady-state drug release for more than 10 days has been attained; this is obviously an important advantage, because the frequency of drug administration is thus reduced.[33]

2.3. Biological metal-organic frameworks

Despite the indisputable and obvious advantages of framework materials as drug delivery containers, an acute problem in this case is cytotoxicity, because these materials can be potentially hazardous for humans. This problem can be avoided by using biological metal-organic frameworks. Materials of this group are composed of biologically significant molecules that have been tested for cytotoxicity and shown to be safe, such as API or other biologically active additives, proteins, peptides and amino acids. Furthermore, if for the previous group (see Table 2), destruction of the material is undesirable, in the case of bioMOFs, this will surely bring no harm to the body, but will lead to release of the biologically active component. The presence of AI in the MOF structure facilitates solution of the synthetic problem, as the target product can thus be obtained in one stage. However, a multistage synthesis including sorption of an AI in bioMOF may enable the simultaneous delivery of several active ingredients. Furthermore, since the biologically active ingredient is

Table 2. Comparison of characteristics of MOF-based delivery systems for anticancer drugs with several popular container compounds (since 2017 until now).

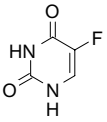
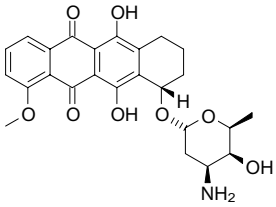
Container compound	Particle size /nm	Surface area /$m^2\ g^{-1}$	Loading efficiency (mass %)	Drug release			Ref.
				medium	amount of the drug (%)	time /h	
5-Fluorouracil (5-FU) 							
Fe-MIL-53-NH_2-FA-5-FAM	120	198	23	pH 7.4	100	25	32
				pH 5	100	20	
FA-IRMOF-3	100		24	PBS	68	96	33
$[Zn_6(L)_3(DMA)_4]\cdot 5\,DMA$	100		21.1	PBS	95.8	96	34
				pH 5	91.6	96	
$\{[H_3O][Cu_6(tpta)_3(DMA)_4(COO)]\cdot$ $\cdot 12\,H_2O\cdot 7\,DMA\}$		1487	47.3	PBS	88	96	35
				Acid	92	96	
CS/Ag-Au	12		19	PBS, pH ~5	67.6	72	36
AmD	68.6	–	31.8	pH 5.0	56	–	37
				pH 6.5	61	–	
				pH 7.4	72	–	
m-MCM-41-NH_2	–	~1000	97	DMSO	99	–	38
MSN	100	1193.19	75	Acid	50	4	39
MWCNTs	863.4		99.8	PBS, pH 7.4	88	16	40
				Acetate buffer, pH 5.0	90	16	
FACS-Mn:ZnS	218		60	pH 7.4	56 – 75	60	41
Doxorubicin (DOX) 							
PD/MNMOF	–		4.3	PBS	95	–	42
ZIF-8-HA	200 – 300		8.9	pH 7.4	9	48	43
P@ZIF-8	85		47.2	pH 7.4	21.1	24	44
				pH 5.0	81.20	24	
				pH 4.2	100	24	
PEG-FA@ZIF-8	185		DOX = 8.9 (Σ = 40.9, DOX + Ver)	pH 7.4	29.8	132	45
HMSN@ZIF-8	360	712.5	50.3	pH 6	17.1	60	46
				pH 5	46.6	60	
				pH 4	71.4	60	
				pH 3	85	60	
MIL/USPIO-cit(10)	130	1.310	14	PBS, pH 7.4	89	25 days	47
Fe_3O_4@MIL-100	10 – 20	2000	19.4	PBS, pH 7.4	38	10 days	48
Fe_3O_4-NH_2@MIL-101-NH_2	140 – 300	96.04	48.8	PBS, pH 7.4	50	–	49
Au-PEG-PAMAM			48.8	pH 7.4	5	96	50
				pH 4	50	96	
AmD	68.6		16.0	pH 5	10	25	37
				pH 6.5	20	25	
				pH 7.4	32	25	

Table 2 (continued).

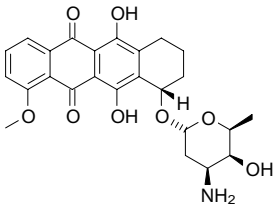
Container compound	Particle size /nm	Surface area /m^2 g^{-1}	Loading efficiency (mass %)	Drug release			Ref.
				medium	amount of the drug (%)	time /h	
Doxorubicin (DOX)							
ZnO QDs	~3		83.4	pH 7.4	36	80	51
				pH 5	72	80	
PAA/SBA-15		356.8	78.6	pH 2	20	–	52
				pH 7.4	64	–	
PMNP	5 – 10		40 – 60	–	–		53

Table 3. Most well-known metal-organic frameworks based on biologically active molecules.

Bioactive molecules	Examples of MOFs/MOF groups	Substrate	Metal	Ref.
Amino acids	ZnBTC	Adenine (ade)	Zn^{2+}	58
(AmAc)	ZnBDC		Zn^{2+}	59
	PCN-530		Zn^{2+}	60
	$(Et_4N)[Cd_3(ade)_2(ipa)_2Br]\cdot 3\,MeOH\cdot 3.5\,DMA$		Cd^{2+}	61
	$(Et_4N)[Cd_3(ade)_2(thb)_2Cl]\cdot 3\,MeOH\cdot 3.5\,DMA$		Cd^{2+}	61
	$Zn_4(5\text{-mtz})_6(AmAc)_2\cdot 2\,(DMF)$	AmAc is L-alanine, D-alanine, L-serine, L-valine	Zn^{2+}	62
Oligopeptides	MPF-2, MPF-9	Z-L-Val-L-Val-L-Glu(OBu^t)OBu^t,	Cu^{2+}, Ca^{2+},	63
		Z-L-Val-L-Val-L-Glu(OH)OH_2	Zn^{2+}	
	CuJAST-1, HKUST-1	Diphenylalanine	Cu^{2+}	64
Proteins [a]	Ferritin MOF	Ferritin	Zn^{2+}, Co^{2+}, Ni^{2+}	64, 65
	ZIF-8	Cytochrome	Zn^2	66
	MOF-74	Myoglobine	Cu^{2+}	67
	$MBPPhen_2$	Cytochrome cb562	Zn, Ni	68
Enzymes	CYCU-4	Trypsin		69
	PCN-333(A)	HRP, microperoxidase-11	Cyt, Al	70
	ZIF-70	Glucose dehydrogenase, methylene green		71
Nitrogenous bases	BioMOF-1	Adenine	Zn^{2+}	72
	BioMOF-100 $Zn_7(ade)_4(BTC)_4(DMF)O\cdot 4\,DMA\cdot 3\,DMF\cdot 4\,H_2O$			73
DNA/RNA	NH_2-UIO-68	siRNA	Zr^{2+}	9
API/AI	$M_2(olz)$, $[Mg_2(olz)(PEA)_2]$	Olsalazine (olz), phenylethylamine (PEA)	Mg, Fe, Co, Ni, Zn	67
	BioMIL-1	Nicotinic acid	Fe^{3+}	74
	$[Fe_3(OH)_y[O_2C{=}C_5H_4N]_5[O_2CCH_3]$	(vitamin B6)		
	BioMIL-2 ($CaO_4OH_2C_5H_6$)	Glutaric acid	Ca^{2+}	75
	BioMIL-3	Azobenzene-3,3′,5,5′-tetracarb-	Ca^{2+}	76
	$[Ca_2(azbz\text{-}TC)(H_2O)(DMF)]\cdot x\,H_2O\cdot y\,DMF$	oxylate (azbz)		
	BioMIL-4 $[Ca(H_2alen)\cdot H_2O]$	Alendronic acid (H_2alen)	Ca^{2+}	77
	BioMIL-5 $[Zn(C_9O_4H_{14})]$	Azelaic acid	Zn^{2+}	78
	$[Zn_3(bdc)_2(dfp)_2]$	Deferiprone (dfp)	Zn^{2+}	79
	$Mg(H_2gal)$	Gallic acid (H_2gal)	Mg^{2+}	80

[a] These protein molecules were associated with the metal-organic framework *via* encapsulation.

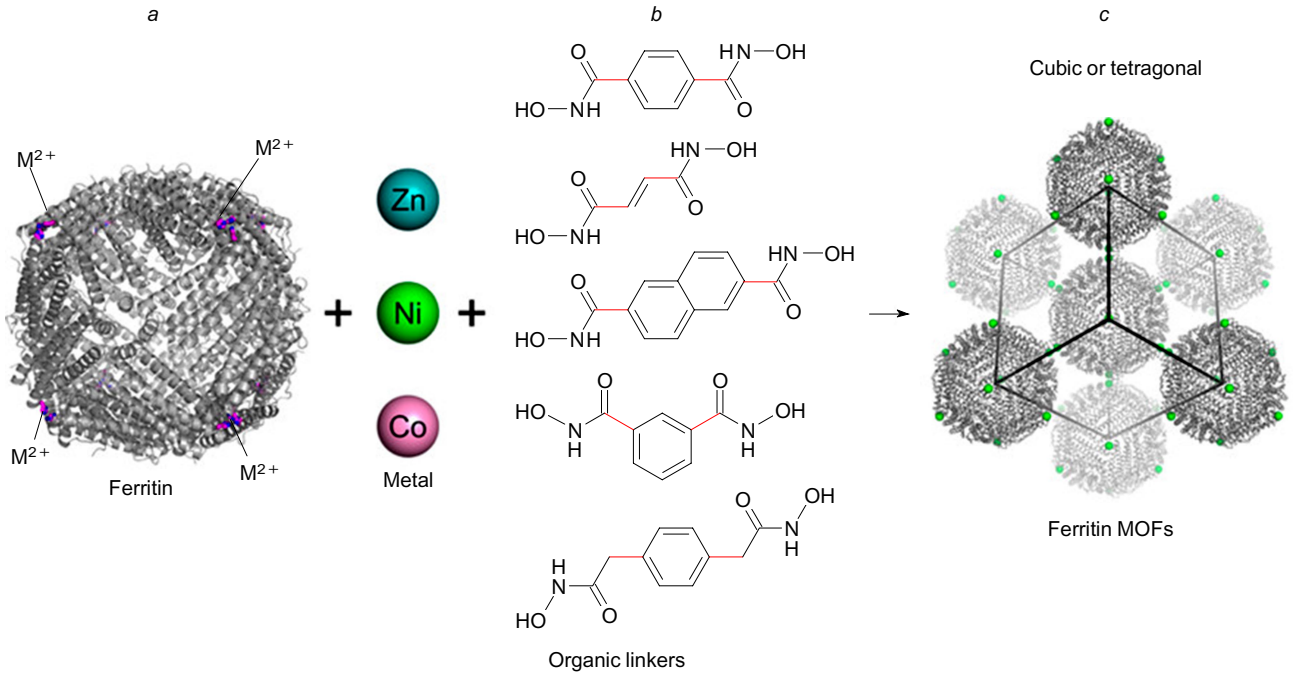


Figure 4. Modular components of ferritin MOFs.[82]
(*a*) Ferritin units; (*b*) ditopic ligands, hydroxamic acid derivatives; (*c*) geometry of the Zn^{II}, Ni^{II} and Co^{II} coordination spheres in the ferritin metal-organic frameworks.

already present in the metal-organic material, a high porosity is not necessary.

It is known that biologically significant molecules with different structures and sizes have been used as ligands for the design of MOFs. This issue is addressed in several reviews, for example, in a review of Imaz *et al.*,[54] who present a broad range of biomolecules used as MOF building blocks, and a recent paper of Rojas *et al.*,[55] which focuses on 3D bioMOFs, their composites and *in vivo* studies of these structures. The above publications consider in detail the morphology of bioMOFs, ranging from description of secondary building blocks of bioMOFs [56] to analysis of the preparation routes and investigation of MOF composites.[57] Therefore, in this review, we intended to shed the light on MOF structures that are most interesting, in our opinion, for the development of drug delivery systems. Brief information about these structures is summarized in Table 3.

Amino acids are key compounds in the biochemistry of living organisms, which also characterizes them as a rather promising class of ligands for the formation of MOFs. Also, amino acids are chiral, thus opening up the way to chiral supramolecular structures; therefore, separation of optical isomers and asymmetric catalysis are equally important applications of these MOFs.

For example, a chiral 3D MOF with a tripeptide as an organic ligand has recently been obtained.[81] The validity of the concept was confirmed by using this MOF for enantioselective separation of methamphetamine and ephedrine. It was shown that solid-state extraction of ephedrine as the target component leads to 50% efficiency of component separation in 4 min.

Considering the synthesis of MOFs with protein molecules as secondary subunits, three structures obtained *via* coordination of the protein ferritin to Zn, Co and Ni metal sites are known.[64, 65] Initially, taking advantage of the high symmetry of this protein complex, the authors were able to generate additional metal sites on the protein surface *via* coordination of Zn atoms to the specially added histidine groups. Thus, zinc-modified ferritin was transformed into a large integrated metal unit for the construction of MOFs. It is of interest that protein MOFs can be prepared both using organic linkers (a set of bidentate ligands was utilized) and without them. In the next publication,[82] the range of protein MOFs was extended by using the fabricated Co- and Ni-ferritin metal units with 5-ditopic ligands (Fig. 4).

Recently, it has been found that crystallization of cyclodextrins with alkali metal salts in the presence of alcohols gives rise to a class of porous metal-organic structures, which have been called cyclodextrin MOFs (CD-MOF) and which can also be classified as bioMOFs. Cyclodextrins (Fig. 5 *a*) are readily accessible, natural, cyclic oligosaccharides, which have occupied long ago their own niche in pharmaceutics, food technology, analytical chemistry and biotechnology. Depending on the number of glucose residues that constitute the ring, the following types of cyclic structures are distinguished: α- (6 units, α-CD), β- (7 units, β-CD) and γ- (8 units, γ-CD) cyclodextrins (Fig. 5 *b*). These molecules have a hydrophilic outer surface able to undergo structural changes and modifications and a hydrophobic inner cavity, which can accommodate diverse biologically active molecules *via* non-covalent interactions and hydrophobic effects;[84] this makes them perfect candidate container structures for such molecules. Development of cyclodextrin-based framework materials resulted in the generation of a new, in principle, class of crystalline 3D materials, CD-MOFs, with several different types of pores: CD cavities

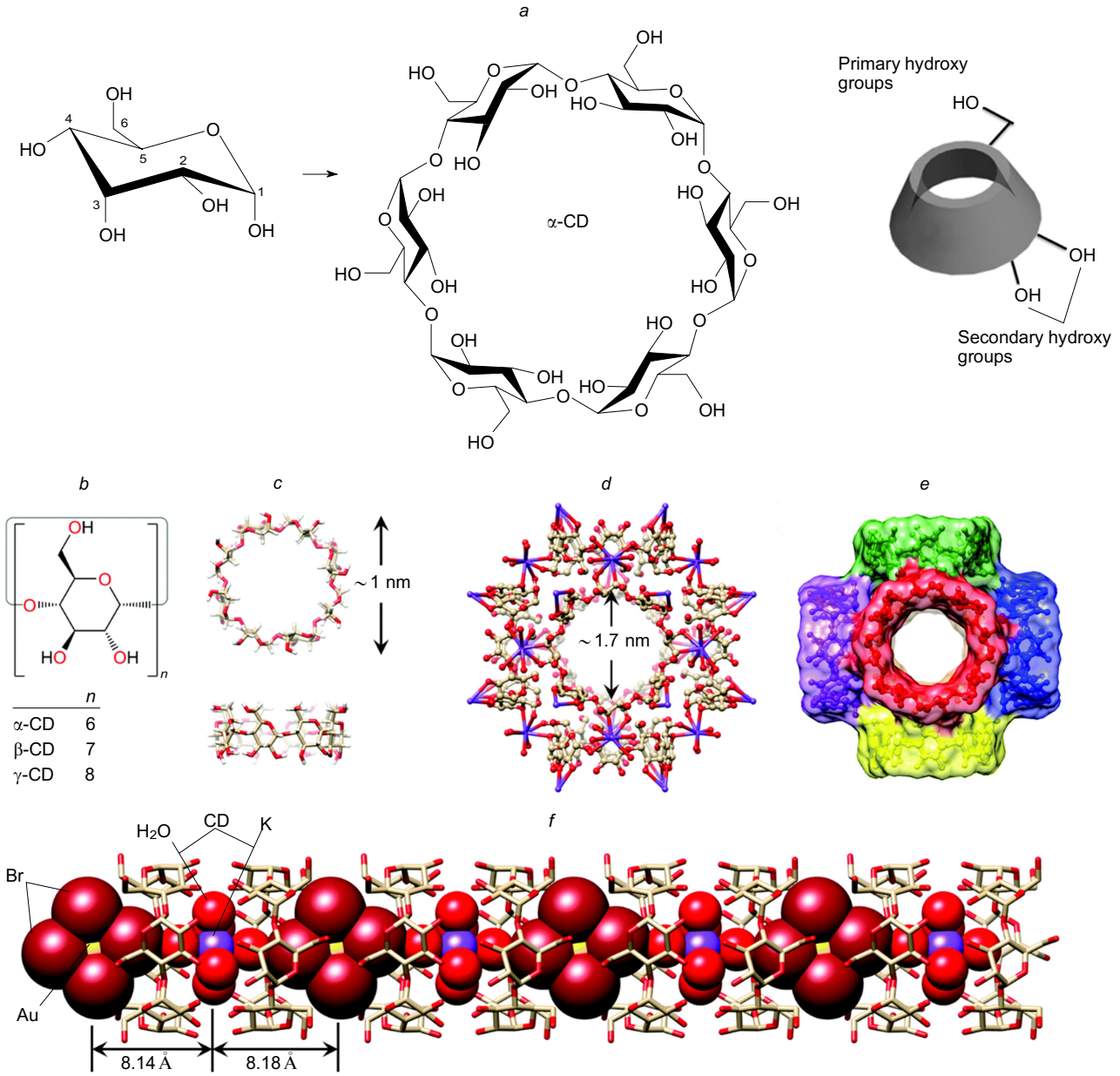


Figure 5. Scheme of formation of α-cyclodextrin (in the middle) from α-D-glucopyranose residues (on the left); schematic model of the α-cyclodextrin molecule (on the right) (*a*),† cyclodextrins (α, β, γ) (*b*), X-ray diffraction structure of γ-CD (side and top views) (*c*), unit cell superstructure of $(\gamma\text{-CD})_6$ in the CD-MOF $[(C_{48}\ H_{80}O_{40}(Rb(OH)_2]_n$ (*d*), cuboidal view of six γ-CD tori (*e*), superstructure of the coordination polymer $\{[K(OH_2)_6][AuBr_4\ ](\alpha\text{-CD})_2\}$ (*f*).[83]

7.5 – 8.3 Å in diameter and CD-MOF pores with an average diameter of 17 Å.

Currently CD-MOFs represent a developing class of framework materials with a large variety of topologies and functionalization options (Fig. 5 *c*). It is also notable that single crystals have been grown for many compounds of this family and their crystal structures have been determined. A typical feature of the crystal structures of these materials is the presence of areas consisting of two conjugated cyclodextrins, which are called dual cyclodextrin units.[85] In many cases, exactly these structural motifs provide strong binding sites for drug molecules.

As indicated by analysis of the literature, despite the considerable progress in the synthesis of bioMOFs, which consists in a large diversity of biologically significant entities used for the framework formation and the final structures based on them (Table 4), there are still a number of points that need to be clarified. For example, because of low symmetry of biological molecules as ligands, it is difficult to apply the known topology screening algorithms to bio-MOF systems, which extremely complicates modelling of

† Taken from J.Q.Sha, Z.H.Zhong, L.H.Wu, A.D.Liu, N.Sheng. *RSC Adv.*, **6**, 82977 (2016).

Table 4. Cyclodextrin MOFs and drug delivery systems based on them.

Name	M^+	CD	Therapeutic agents	Loading (mass %)	Ref.
CD-MOF-1	K^+	γ-CD	Captopril	12.59	84
			Lansoprazole	12.07	86
				23.2	87
			Ibuprofen	13	86
				26	88
			Fenbufen	19.6	89
			Sucralose	27.9	90
Na-α-CD-MOF	Na^+	α-CD	5-Fluorouracil	8.5	91
			Methotrexate	38.15	91
			Silibinin	12.8	91
			Ferulic acid	10.87	91
			Quercetin	32	91
Na-β-CD-MOF	Na^+	β-CD	5-Fluorouracil	23.2	92

their self-assembly. In addition, in the case of large entities such as proteins, it is difficult to predict whether or not the active sites of these molecules would be accessible after their incorporation into MOFs.

Studies of MOFs are often associated with the problem of hydrolytic stability. Nevertheless, many MOFs that are relatively stable in water have been reported.[93] In particular, such stable structures are encountered among Zn-containing ZIFs. For example, a ZIF-7-based membrane for gas separation[94] is hydrolytically stable for 50 h. The H_2 and CO_2 permeability decreased during the stability assay by 10%, whereas the separation factor did not change.

Approaches for increasing the material stability in aqueous media have been developed; one of them includes cross-linking of functional groups, which increases the hydrophobicity of the framework. Thus, active research along this line is in progress and new solutions are being continuously developed.

2.4. Biocompatibility of metal-organic frameworks

Riding on the popularity wave of MOFs as drug delivery agents, numerous new framework materials have been developed, parameters of drug loading into framework cavities have been verified, and the drug release from MOFs has been evaluated. However, the issues of biocompatibility and destruction of materials in biological media are not entirely clear and require further research, data accumulation and subsequent data analysis.

The biomedical application of new materials imposes certain requirements on the design of new drugs and dosage forms. Therefore, it is very important to provide an appropriate dose to obtain the desired therapeutic effect, while minimizing harm to the patient. Indeed, due to the presence of metal sites in MOFs, it is necessary to select the metal considering its toxicity. In particular, iron and zinc are present in the body in relatively high concentrations and have high half-lethal doses (LD_{50}) (Table 5), which makes them most popular for the development of new MOFs. Any compound or element should be checked for biorelevance using Bertrand's diagram,[96] which establishes the relationship between the deficiency in the body, the optimal physiological response and toxicity depending on the administered dose. However, toxicity also depends on other factors such as the administration route, exposure time and time of accumulation/elimination from the body. Therefore, even the elements and compounds that are considered to be toxic, may have therapeutic effect when used in micro and nano quantities. On the other hand, metals that are usually classified as non-toxic may be hazardous when present in large quantities.[55]

Table 5. Toxicity of the most widely used components of metal-organic frameworks.[55,95]

Element	Average composition in humans /g	LD_{50} for rats /mg kg^{-1}
	Metal cations	
Al	–	200–1000
Au	$42-420\times10^{-9}$	–
Bi	0.0005	⩾2000
Ca	1000	1940
Co	0.003	691
Cr	–	50–150
Cu	0.072	30
Fe	4–5	450
K	140	3020
Li	0.007	590
Mn	0.012	1484
Mg	1.9	5000
Zn	2.3	100–600
Zr	–	4100

Ligand	LD_{50} for rats /mg kg^{-1}
Organic linkers	
Terephthalic acid	5000
Trimesic acid	8400
Naphthalene-2,6-dicarboxylic acid	5000
1-Methylimidazole	1130
2-Methylimidazole	1400
Isonicotinic acid	5000
5-Aminoisopthalic acid	1600

The choice of organic linkers is dictated by their half-maximal inhibitory concentration (IC_{50}),[97] which can be

determined in *in vitro* studies in cell lines. Endogenous organic molecules are usually preferred as they are biocompatible. For example, the amino acid histidine contains an imidazole moiety, which is also used in ZIFs; therefore, imidazole derivatives can serve as MOF ligands.

Several *in vitro* studies of the MOF toxicity have been reported. A standard experiment for such studies is the MTT assay,[30] measuring the effect of both TA-loaded and TA-free MOF particles on various cell lines. The MTT assay,[98] which was first described more than 30 years ago, is widely used for cell survival assays and is included in most molecular biology and medicine protocols.[99] The test is based on the reduction of a tetrazolium yellow dye [3-(4,5-dimethylthiazol-2-yl)-2,5-diphenyltetrazolium bromide] with mitochondrial dehydrogenases of living cells to purple formazan crystals, which are insoluble in the aqueous medium of cell habitation. The formazan crystals are dissolved in DMSO or in an HCl – isopropyl alcohol mixture and are quantified by colorimetry. During this procedure, living cells are destroyed, *i.e.*, the MTT assay is destructive. Furthermore, the MTT assay for cytotoxicity is poorly applicable to cases where suspended cell cultures are used, because it implies complete removal of the culture medium at the stage of dissolution of formazan crystals. Nevertheless, benefits of this method include economic feasibility and excellent reproducibility of the results.[100] In addition, this method can be used to monitor the decomposition of the material and the release of the drug.

Experiments in which MOF particles were delivered directly to the cells were carried out for various cell lines such as rat embryonic fibroblasts (REF52WT),[101] non-small cell lung cancer cells (NCI-H292), human breast cancer cells (MCF-7), human acute myeloid leukaemia cells (HL60),[102] human colon adenocarcinoma cells (HT-29),[103, 104] human leukaemia and human multiple myeloma cells,[105] canine endothelial sarcoma cells (FITZ-HSA),[106] human cervical carcinoma cells (HeLa [107]) and murine fibroblasts (NIH/3T3).[108]

The cell viability, efficiency of malignant cell killing through apoptosis, targeted delivery of particles to the cell, and MOF uptake by various cells *via* endocytosis have been studied in considerable detail. The conjugation of targeted moieties to MOFs enhanced the delivery of loaded drugs and helped to detect damaged cells or tissues (targets), such as for example, cancer cells. The targeted molecules used for this purpose include various affinity ligands, peptides, oligonucleotides, antibodies, drugs and biologically active compounds, which ensure the binding of the particle to target markers on the cell surface.[109]

It is noteworthy that, despite its significance, the number of publications devoted to the *in vivo* effect of MOFs is still moderate.[110] Mohamed *et al.*[111] studied the impact of MIL-89 and poly(ethylene glycol)-coated MIL-89 nanoparticles on rats. The authors concluded that these compounds are applicable in drug delivery systems and are not hazardous to humans. In another study, three carboxylate MOFs based on Fe^{III} cations were intravenously administered to rats in high doses (up to 220 mg kg^{-1}).[112] The animals were observed for three months, and the toxicity was estimated from the behaviour of animals, change in the body weight, water and food intake, and results of histopathological examination (liver, spleen, heart, lungs, brain and kidneys) and biochemical studies. The particles were accumulated in the liver and spleen, but no signs of histological or functional changes were noted upon their progressive degradation and elimination of excess iron and metabolized exogenous ligands.

In yet another study, *Danio rerio* fish was chosen as a subject for toxicity studies.[113] The introduction of Zn-based 2D MOFs in concentrations below 125 μg ml^{-1} over a period of 24 h and below 62.5 μg ml^{-1} over a period of 48 h did not induce notable morphological changes in comparison with the control group. These results indicated that this MOF in these concentrations is not toxic to the given species.

A recent study on the *in vivo* toxicity of Gd^{III}-based MOF nanoparticles after intravenous administration to mice showed no deviations of the biochemical blood values. Only minor changes in the state of liver associated with particle accumulation were detected.[114]

An important characteristic of MOFs (except bioMOF) is the size of the obtained crystals. From the standpoint of medical applications, nanometre-sized MOFs (often called nano metal-organic frameworks, NMOFs) are efficient. The particle size of NMOFs ranges from tens to hundreds of nanometres, with the structural diversity and physicochemical properties inherent in bulk MOFs being retained.[115] An inappropriate choice of the dispersion properties of the material can not only reduce the efficiency of the drug, but also induce serious toxicity-related problems. This can be illustrated by the fact that intravenous administration requires stable suspensions with rather small ($\leqslant$200 nm) uniform particles in order to avoid fast particle aggregation or precipitation, which could cause severe embolism.[116] The particle size also affects the metabolic pathways. For example, relatively small nanoparticles (20 – 30 nm) are usually eliminated *via* renal excretion, whereas larger particles (30 – 300 nm) can be rapidly taken up by the cells of mononuclear phagocytic systems and are mainly encountered in tissue macrophages (of mainly liver and spleen).[117, 118] Also, the particle size and the surface properties of MOFs markedly influence penetration of various barriers on the way toward the target and, hence affect, the biodistribution and efficiency of their biological action.[119]

Metal-organic frameworks are sophisticated multilevel materials. This is reflected in the properties and characteristics of these compounds and brings about the necessity to use dedicated methods for their investigation. It is noteworthy that drug-loaded MOFs are three-level composite materials. Any subsequent modification such as particle coating with polymers, biomineralization and so on increases the number of levels in the system and, hence, makes the system more sophisticated. Therefore, the kinetic and thermodynamic aspects of the MOF-based drug delivery systems are quite ambiguous and complex for description. Different theories may be efficient for the description of processes taking place in different systems, and correct and most comprehensive understanding may be provided by the use of several models.

Due to these difficulties, there is a pressing need to streamline the work and rationalize the stages of design of MOF-based drug delivery systems. Materials of this type are promising candidates for application of the rational design concept. This approach, which was first established as an important tool in biology and biomolecular engineering and proved to be efficient in the development of TAs, is currently becoming more and more popular in materials science. Rational design is the strategy of development of new

materials with a desirable functionality based on the ability to predict, relying on physical models, how the structure of a molecule would affect its behaviour. This is usually achieved by means of computer simulation, the role of which in the context of the design of MOFs and MOF-based drug delivery systems is discussed in the next Section.

3. Computer simulation for the rational design of MOF-based materials for targeted drug delivery

The use of computer simulation in the design of new materials has markedly extended the methodologies used for their design. Computational methods can serve to optimize and guide the experiment from the initial stages to the completion.

As applied to the design of drug delivery systems, computer simulation can be used to study the self-assembly,[120,121] structural and dynamic characteristics of the obtained aggregates,[122,123] drug loading capacity,[122–125] distribution and localization of TA molecules in the container cavity,[126,127] stability of TA–container complexes,[126,128] mechanisms and rate of TA release[129] and competitive sorption and release in drug delivery systems[130,131] and to develop or optimize the possible targeted delivery.[132] In addition, computational methods make it possible to evaluate the role of environment conditions such as pH, temperature, type and concentration of salts present in the biological medium, the nature of counter-ions,[127,133] external stimuli such as magnetic fields[134,135] or interaction with other biomolecules (such as serum proteins, siRNA, heparin).[136,137]

Currently, the key approach to the development of new functional materials is based on the rational design concept. In the context of medicinal chemistry, this implies predictive modelling of new compounds possessing certain functionality. In the English-language literature, this has long been termed as 'computer-aided drug design' (CADD) (Fig. 6), which implies the use of computer simulation in the drug design.[138] The capacity of this method is not limited to screening of potential therapeutic agents and most promising structural units for the design of drug carriers; the method is also suitable for predicting the possible derivatives of the developed compounds and for modelling TA interaction with components of the environment and TA metabolic pathways. Most often, CADD is utilized to solve three global tasks: (1) considerably reduce the search domain for desired molecules and identify the most appropriate candidates for experimental studies; (2) search for new, more efficient derivatives of known compounds; (3) develop modification pathways for known therapeutic agents and platforms in order to increase the bioavailability, stability and other parameters.

Although conventionally the CADD-based approach mainly targets the search for new active candidate pharmaceuticals, in the context of modelling of drug delivery systems, CADD is also an important tool for determining the mechanism of binding of a drug molecule to a receptor and drug affinity, *i.e.*, the mechanism of TA action.[139] To perform the pharmacological function, a therapeutic agent

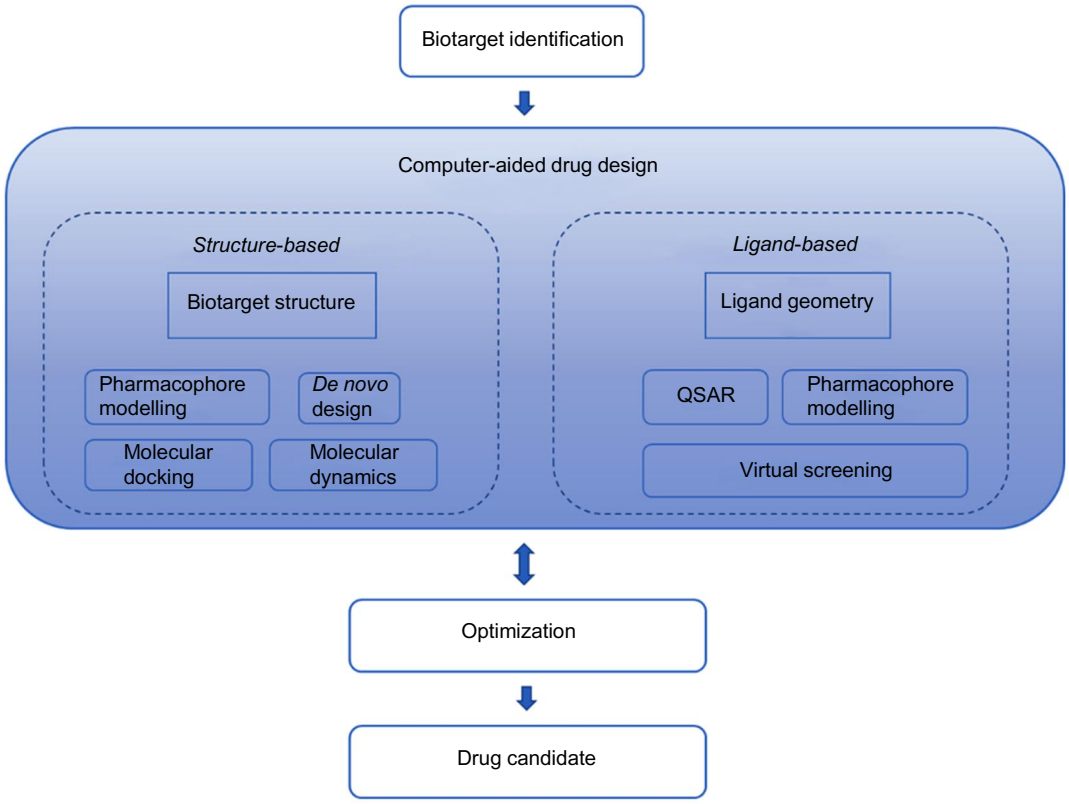


Figure 6. Diagram depicting computer-aided drug design/search for new drugs.[138]

has to interact *in vivo* with a particular substrate ligand. It is known that receptors are biological structures responsible for binding of the therapeutic agent at the cellular level.[140] Most often, receptors are complex protein molecules. Binding of TA to receptor may occur *via* the same interactions as binding to the delivery container, namely, *via* the hydrophobic and electrostatic interactions and hydrogen bonds.[141]

3.1. Screening of framework materials

The structures of drug delivery systems are complex and hierarchical; therefore, the same features are inherent in the computer simulation of these systems. The minimum set of modelling elements comprises three objects: the TA, the TA container and the medium in which the TA/container system will interact (for the convenience, the latter will be denoted biomedium). Therefore, before simulating the system operation as a whole, it is necessary to solve a number of primary problems that bring us closer to the understanding of how the system function. In particular, it is crucial to (1) resolve the container structure and determine interaction parameters between the container and the medium, (2) understand the mechanism of TA action and (3) estimate the strength of the interaction between the TA and the container. Thus, computer simulation of functioning of drug delivery systems based on framework materials is a many-objective labour-intense problem.

Framework materials are sophisticated ordered structures consisting of repeating subunits and belonging to the subject matter of reticular chemistry; hence, the search for new configurations is a priority task for the development of this area. In the context of application of framework materials as drug containers, the possibility of fast and efficient adjustment of the framework structure to a definite type of drug may considerably facilitate screening of drug delivery system components. This is due to the fact that in the case of any difficulties in the delivery system design such as inefficient drug sorption, too fast drug release and so on, it would be more easy and efficient to change the container rather than the API. A way out of this situation is provided by isoreticular frameworks (IRMOFs). However, enumeration of all possible configurations will take an enormous amount of time.

A software program aimed at the targeted search for such structures is AuToGraFS (Automated Topological Generator For Framework Structures).[142] This program performs the search for both periodic and non-periodic systems proceeding from the known bond topologies. The AuToGraFS program can be used as either autonomous software or a module in the Python Atomistic Simulation Environment (ASE).[143] In this environment, AuToGraFS is by default connected to the UFF4MOF force field[144] for fast geometry optimization of the modelled structure. In general, the approach comprises the following stages: the initial topology is specified and boundary conditions are imposed; the topology is scaled and a periodic model with definite slots for the framework building blocks is generated; the slots are filled with the building blocks *via* geometric operations; the connections between the blocks are generated taking into account the known topologies (defective units are eliminated); and the structure is derived and optimized using a force field. A successful example is MIL-53 in which the central Cr atoms were replaced by Al (Fig. 7). Good agreement between theoretical and experimental data is observed (Table 6); visualization of this structure is presented below in Fig. 13 *a*.

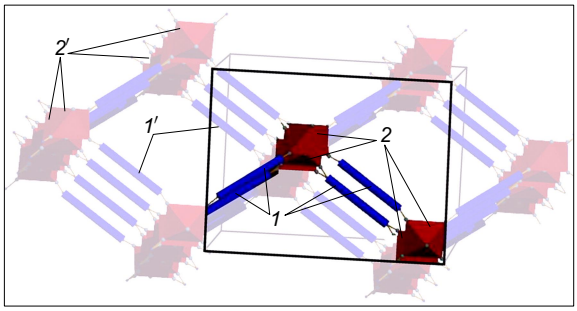


Figure 7. Unit cell used to generate MIL-53 analogues.[142] The four ditopic linkers (*1*) and four metal sites (*2*) are the objects located in the AuToGraFS field. (*1*′, *2*′) Periodic images.

Table 6. Unit cell parameters of MIL-53 determined experimentally and calculated by AuToGraFS.[142]

Unit cell parameters	Calculated values	Experimental values	Error (%)
a	6.213	6.812	−8.8
b	16.124	16.733	−3.6
c	13.231	13.038	1.5

In the case of extended conjugated polymeric structures such as MOFs, the use of building blocks for simulation is a reasonable approach. For example, structure selection based on building blocks was shown to be efficient for the search for frameworks for gas separation.[145 – 149] This approach can serve as a good example of successful screening, which would enable in the future screening of MOF-based drug containers.

However, this approach is limited, first of all, because the reference points used in the modelling are the already known structures, which are not subsequently subjected to significant changes, and this may result in minor changes in the properties of materials. A recent review[150] describes the steps towards the next level of the computational screening of structures. In particular, screening based on modelling of new building blocks rather than on the search through the Cambridge Structural Database (CSD) has been proposed.[151] This method is known as the automated assembly of secondary building units (AASBU).[152]

The secondary building units are randomly distributed in the unit cell and specify the points of interaction at which they can be connected to other building units. These connection sites are parameterized, in order to promote or disfavour the connection of certain units. The simulated annealing algorithm is used to rearrange the structural units. At each stage, the cell size and the distances between the units are allowed to vary to relieve interatomic contacts. One run usually yields $\sim 10^4$ primary configurations. Radial distribution functions and simulated diffraction patterns are used to identify duplicates, which are then removed. The geometry of the configurations is then optimized and systems with non-optimal energy values are eliminated. This gives rise to a

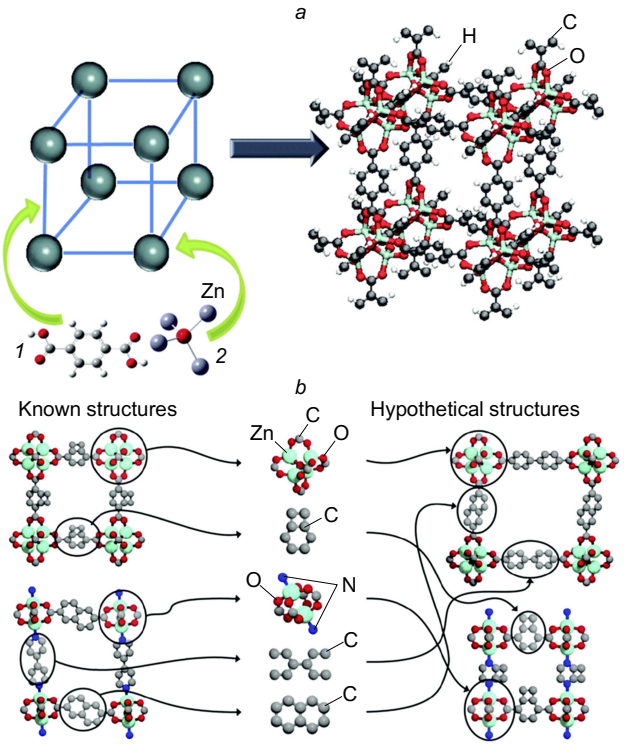


Figure 8. Diagram of the top-down approach (*a*). In the bottom-up approach, the building blocks are extracted from real MOFs and rearranged into new combinations to generate hypothetical frameworks (*b*).[150]
A terephthalic acid molecule is shown as the ligand (*1*), the metal unit is Zn_4O (*2*), which is located at the lattice points to form MOF-51.

few hundred possible configurations of building units, which are ranked according to the connection strength.

As an alternative to the energy minimization procedure used in the AASBU method, geometric approaches have been developed. They can be classified into two large groups depending on the screening algorithm, that is, top-down and bottom-up approaches. The bottom-up approach implies successive connection of known building blocks until a periodic crystal structure is generated. The top-down approach proceeds from a specified network or topology and then the search for appropriate building blocks, which are structure-forming elements in this network, is carried out. In addition, these methods can be used to predict structures containing more than one linker.[153] These approaches to structure generation are depicted in Fig. 8.

A new trend in the development of framework materials, which is gaining attention, is the functionalization of known structures and targeted screening of multifunctional frameworks. For example, new systems called multidimensional or heterogeneous MOFs are distinguished. The formation principle of some materials is a combination of several functional groups or active sites in order to endow the final material with certain properties.[154] One way is to use functionalized linkers in the synthesis.[155] Another approach to the synthesis of these materials is the preparation of heterometallic MOFs, that is, frameworks with cations of different metals in the inorganic nodes.[156]

Coudert's research team [157] developed a strategy based on density functional theory (DFT) calculations meant for investigation of heterometallic MOFs and able to predict whether the pre-specified combination of metals would induce clustering and formation of a new material, or the cations would be randomly distributed. The calculations were carried out for two bimetallic MOFs, MOF-5 and UiO-66,[156] using the CRYSTAL14 program.[158] This program is able to carry out electronic structure calculations on periodic structures using localized atom-centred basis sets

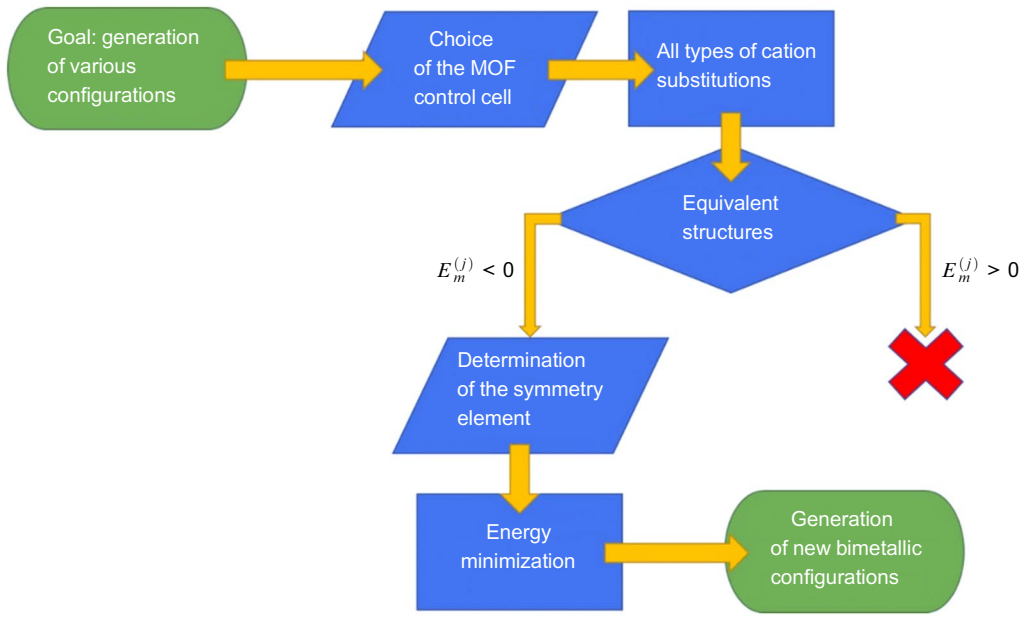


Figure 9. Block diagram for generation of various framework configurations (based on Ref. 157).

that take account of the crystal structure symmetry. The B3LYP functional was chosen for the MOF-5 structure [159] and the PBEsol functional was applied to the UIO-66 family.[160] Grimme's dispersion correction was used in the calculations.[161] The bimetallic units were modelled by means of the tools for description of solids with disorder and solid solutions implemented in the CRYSTAL14 software. The generation of configurations is illustrated in Fig. 9.

Analysis of the stability of bimetallic configurations with respect to homometallic ones performed by comparison of the mixing energies has served as the criterion for the rejection of non-optimal structures. For a model framework with element A being replaced by element B with the number of units j ($1 \leqslant j \leqslant p$) and the rate $x_j \in [0; 1]$, with the energy after relaxation given as $E^{(j)}$, the mixing energy is defined as

$$E_m^{(j)} = E^{(j)} - x_j E_B - (1 - x_j) E_A \quad (1)$$

where E_A and E_B are the energies of homometal frameworks. A negative value of E_m indicates that the framework with this crystal structure is energetically more stable than those of the homometallic analogues (for $T = 0$ and $P = 0$).

Other important parameters are topological indices,[162] the distances between metal cations and ligand functional groups bonded to the metal cations and the Mulliken charges.[163]

3.2. Modelling of the sorption of drug molecules in the framework cavities

The design of drug delivery systems based on framework materials is based, most often, on the adsorption of drug molecules in the framework cavity. Hence, understanding of the adsorption and formation of the sorption complex is key to further development and studying of these materials. Computer simulation is an indispensable tool providing both qualitative and quantitative (with the modern level of computational chemistry) description of the sorption process. Depending on the level of the problem, an appropriate simulation method should be chosen out of a large variety of approaches differing in the accuracy and dimensionality. Usually, it is possible to draw a correlation between the system size and the computation accuracy and also the time of simulation (Fig. 10). For example, empirical force fields are applied to simulate the processes taking place during long periods of time involving systems consisting of thousands of atoms.

Description of the reactivity and interactions between the drug and framework materials, which bring about the bond cleavage and other significant changes in the electronic

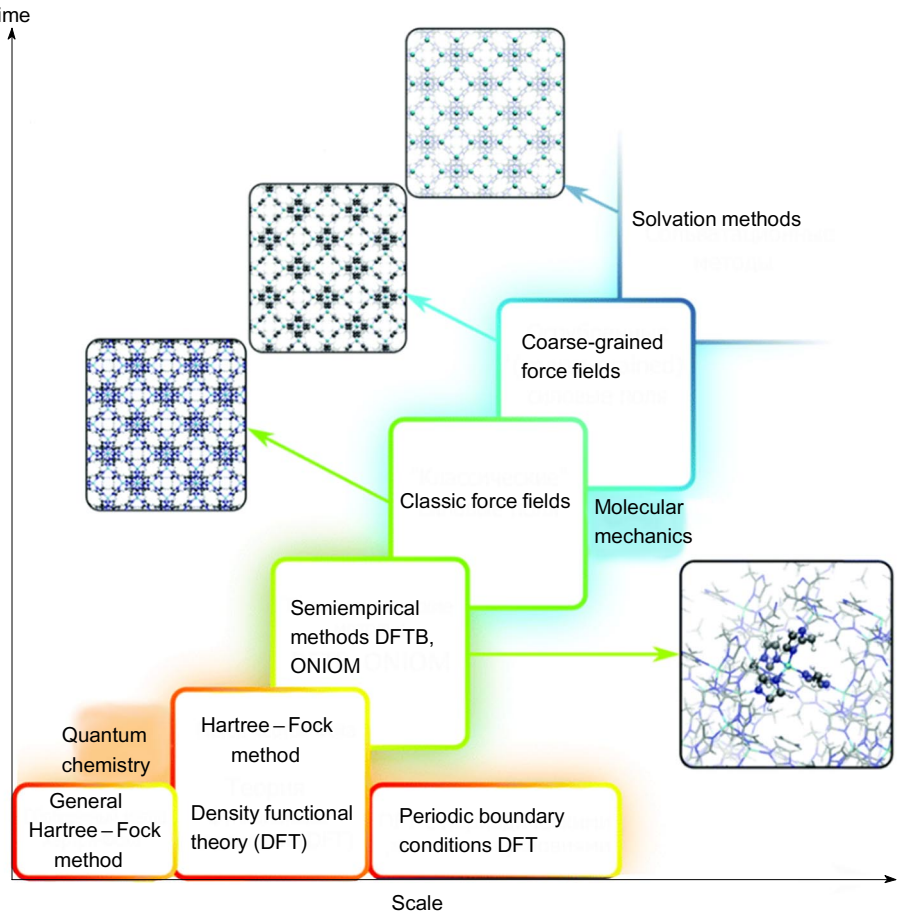


Figure 10. Hierarchy of compuational methods.[164]

structure such as recoordination in the MOF metallic unit requires the use of quantum chemistry methods.

3.2.1. Quantum chemical calculations

Owing to the optimal combination of accuracy and relatively short computing time required with modern computers, methods of density functional theory have found wide use in the modelling of MOFs.[165] The key issue is the choice of the exchange-correlation functional (below referred to as just functional) to express the dependence of the potential energy of a multielectron system on the electron density at a specified set of approximations and parameters.

Currently, there exist quite a number of functionals with different approximations and many basis sets, which can be combined in different ways to select computational schemes for particular cases. Nevertheless, certain trends for computational schemes have been formed for addressing framework materials as drug delivery systems. For example, local density approximations (LDAs) are currently no longer used, being replaced by generalized gradient approximations (GGAs), which still remain a popular group of exchange-correlation functionals (PW91,[166] PBE [167]).

Among basis sets, the def2-XVP family of basis sets [168] (X = S, TZ, QZ, *etc.*) is often employed which covers most of the Periodic Table. The previous generation, def-XVP [169] (X = S, TZ, QZ) or Pople basis sets [170] (6-31G, 6-311G, *etc.*) are also used in the context of DFT calculations. An advantage of computations with the def2 basis sets is that it is possible to apply RI-J, RI-JK and RIJCOSX approximations, which considerably reduce the required computing time.[171] Also, the numerical DNP basis set [172] is often used; this reduces the basis set superposition error, which is rather important for modelling of adsorption and intermolecular complexes.[173]

The DFT simulation of framework materials is often carried out with periodic boundary conditions using the plane wave basis sets. This is done by means of GGA functionals (Table 7). For example, periodic DFT calculations have been successfully employed to model MOFs of the MIL, UMCM, HKUST, ZIF and TTI-COF families.[8, 174 – 183]

Table 7. Examples of DFT simulation of framework materials.

MOF	Method	Functional/basis set (additional approximations)	Goal	Ref.
IRMOF-16 OH-IRMOF-16	PM7 DFT-D3	PBE/def2-TZVP + (CP correction)	Studying the TA – MOF interaction	174
IRMOF-14 IRMOF-16	DFT	PBE/def2-TZVP SCS(MI)-MP2	Estimation of the drug binding energy, drug and MOF geometry optimization	175
IRMOF-74-III OH-IRMOF-74-III	PM7 DFT-D3	RI-PBE/def2-TZVP	Identification of preferable sites for sorption and analysis of the nature of interactions between the drug molecule and MOF	176
MIL-101(Cr)	Periodic DFT calculations	PW91/DNP	Geometry optimization for sorption complexes	177
MIL-53(Fe)	The same	PW91/DNP	The same	8
MIL-53-H MIL-53-Br MIL-53-NH_2	"	PBEsol/PAW DFT + U	Initial geometry optimization for MOF and drug molecule. Estimation of the decrease in the pore volume upon drug encapsulation, determination of the geometry of drug molecules in the framework cavities and calculation of the drug binding energy	178
MIL-53(Fe)	"	PW91/DNP	Geometry optimization for the crystal unit cell, interaction between the drug and the framework	179
MIL-101 UMCM-1	DFT	B3LYP/LANL2DZ	Identification of lowest energy conformations (DFT calculations), determination of atomic charges on the MOF (ESP method)	180
HKUST-1		PBE/def-SV(P)//B3LYP/TZVP	Geometry optimization for sorption complexes. Interaction energy between drug molecules and unsaturated metal units	181
ZIF-7, ZIF-8 and ZIF-9	DFT	B3LYP/6-311**G ChelpG	Calculation of atomic charges	182
TTI-COF		PBE0-D3/Def2-SVP (CP correction), PBE0-D3/Def2-TZVP (CP correction), PBE0-D3/Def2-SVP//B97-3/pcS-2	Geometry optimization for the initial compounds and sorption complexes, determination of the interaction energy, signal positions in the NMR spectra	183

The application of DFT to the development of drug delivery systems can be exemplified by a study of binding of the anticancer drug tamoxifen to the functionalized organic linkers of the IRMOF-14 and IRMOF-16 frameworks functioning as MOF elementary building blocks.[184] The main types of interaction between the drug and the linkers include hydrogen bonds and π – π interactions. The strength of these types of bonding characterizes the efficiency of operation of the whole system and, what is most important, indicates whether the controlled drug release is possible. The study was carried out by DFT calculations at the GGA level of theory using the SCS(MI)-MP2 method.[185] The interaction energies of tamoxifen with organic linkers were determined by scanning the potential energy surface considering different orientations of the drug molecule in the system. This gave the values of maximum interaction energies (16.6 kcal mol^{-1} for IRMOF-14 and 18.32 kcal mol^{-1} for IRMOF-16) (Fig. 11). These binding energies are optimal for drug sorption and delivery without attachment in the framework cavity, whereas higher binding energies would prevent drug release inside the body in due time. This subject matter was further developed in another publication [175] in which the presence of glycine was taken into account and the strength of non-covalent interactions of the framework elements was calculated.

A research team [178, 186] used the density functional theory to identify the preferable caffeine binding sites in the cavities of zirconium MOFs. The authors proved that metal atoms are not strong binding sites, while caffeine is preferably adsorbed near the organic linker. The binding is mainly due to hydrogen bonding between a caffeine oxygen atom and the carboxyl group of the linker. Also, weak van der Waals interactions (CH-π-type) between the methyl groups of the drug molecule and the organic part of the matrix were also detected. Low drug loading was explained by strong competition with the solvent (water).

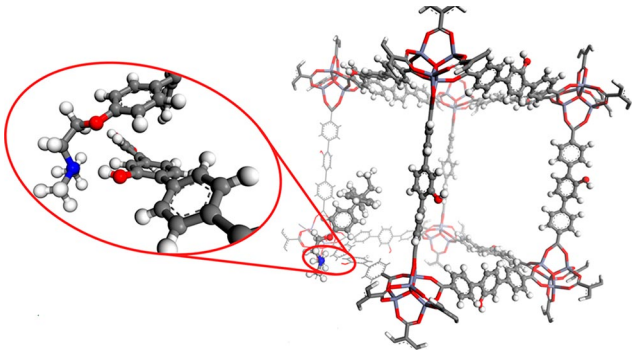


Figure 11. Site of interaction of OH-IRMOF-16 with tamoxifen.[184]

Of considerable interest is a study [181] dealing with the interaction of biologically significant organic molecules such as caffeine, niacin, urea and glycine with the copper-based HKUST-1 framework containing coordinatively unsaturated metal sites. In all calculations, the authors used the third-generation Grimme's dispersion correction (D3). Also, the thermodynamic parameters of adsorption were calculated. Estimates were made of molecule binding directly to the metal site and sorption within the MOF pore, with both large and small cavities being considered. The

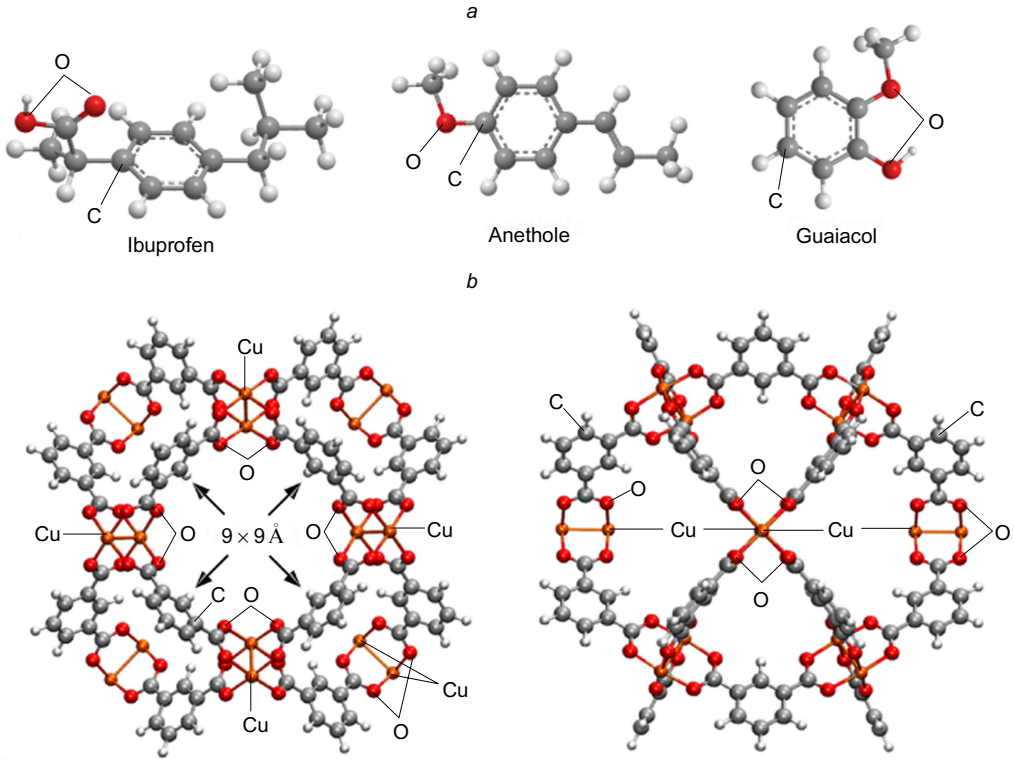


Figure 12. Ball-and-stick models of ibuprofen, anethole and guaiacol (*a*); structure of HKUST-1 with pore size of 9 × 9 Å (*b*).[183]

adsorption enthalpy (ΔH_{ads}) was calculated by the following formula:

$$\Delta H_{ads} = IE + \Delta ZPE \quad (2)$$

where IE is the electronic interaction energy, $\Delta ZPE = ZPE_{(MOF\cdots guest)} - ZPE_{(guest)}$ is the zero point energy in the harmonic approximation.

The electronic interaction energy was calculated by the hybrid high-level/low-level (HL/LL) scheme with allowance for the basis set superposition error, which is rather significant for estimation of the non-covalent interaction energy with Gaussian basis sets being used.

According to calculations, the interaction with metal sites proved to be the strongest for all organic molecules. Interesting results were obtained for the adsorbate – adsorbate interaction strength in the case of TA adsorption in the pores. For high loading of guest molecules (caffeine, urea or glycine), dimerization energy was found to be higher than the adsorption energies. Thus, these molecules are expected to be dimerized and/or trimerized instead of being adsorbed in the pores.

Chen *et al.*[187] investigated the sorption of ibuprofen, anethole and guaiacol molecules in the HKUST- 1 cavities (Fig. 12) and confirmed the possibility of prolonged release of these drugs, which is critically important for functioning of the drug delivery system.

It is necessary to emphasize the importance of balanced description of all types of physicochemical interactions for the framework materials by quantum chemical methods. In this case, apart from covalent interactions, non-covalent interactions such as hydrogen bonds, $\pi - \pi$ contacts and van der Waals forces must be adequately described. The DFT methods, are currently the state of the art in the field, do not take into account the non-local electron correlation and, hence, they are inapplicable to modelling of $\pi - \pi$ interactions and van der Waals forces and they also require dispersion corrections.[188 – 190] Exceptions are provided by non-local functionals specially developed for describing dispersion interactions, such as VV10 (Ref. 191) or vdW-DF.[192]

Even at the current level of development of computers, modelling of structurally complex systems consisting of components of different nature and hundreds of atoms by quantum chemistry methods, in particular, by DFT methods, is far from being a routine problem. Therefore, methods requiring less computer resources are demanded.

3.2.2. Monte Carlo method

Force field-based and Monte Carlo methods are often preferred for description of adsorption processes in the cavities of framework materials or other meso- or microporous materials. There are two most popular algorithms for such calculations, namely, the Metropolis algorithm[193] and the configurational bias algorithm.[194]

The Metropolis scheme comprises the following stages: generation of new configurations of sorbed molecules and calculation of their energies; comparison of the energies of starting and new configurations; and energy comparison in terms of the Boltzmann distribution. If the generated system is more probable according to the Boltzman distribution, this step is accepted; if not, the system returns to the initial state.

The configurational bias Monte Carlo algorithm[194] is based on the scheme developed by Rosenbluths in 1955.[195] The key principle of algorithm operation is the check of new configurations generated by the title procedure for the compliance with the Rosenbluth statistical weight. The configurational bias Monte Carlo algorithm is implemented *via* the following stages: (1) generation of the trial configuration in the system by addition of a new molecule or its part according to the Rosenbluth scheme and calculation of the Rosenbluth statistical weight for the updated system; (2) determination of the Rosenbluth weight factor with respect to the previous configuration; (3) acceptance of the algorithm stage with a certain probability.[196] In the modelling of adsorption, the adsorbate molecules fill the cavities *via* change in the positions of atoms (removal/filling) with the goal to find the most energetically favourable conformations, while avoiding overlap with the positions of other molecules.

An early study in which the Monte Carlo method is used to evaluate the efficiency of drug loading into biocompatible MOFs and to develop screening methods for MOFs as drug delivery agents was reported by Bernini *et al.*[197] Using this method, the authors modelled the sorption of the nonsteroidal anti-inflammatory drug ibuprofen in biocompatible MIL frameworks [MIL-53(Fe), MIL-100(Fe), MIL-101(Cr)] in the grand canonical ensemble. Also, this approach was applied to MOF-74(Mg),[198] CD-MOF with hydrocarbon linkers[199] and bioMOF-100 with an extensive surface area (4.300 $m^2\ g^{-1}$).[200] The major benefit of this approach is the possibility to evaluate both drug adsorption and attachment in the pores and the drug release. In addition, it was shown that the Monte Carlo method discloses the mechanism of drug adsorption in the pores. In particular, by calculation of the radial distribution function for the system, the authors described the interactions between the framework metal atoms and the ibuprofen carboxyl group as well as hydrogen bonding between the donor hydrogen atoms of the ibuprofen carboxyl group and the acceptor oxygen atoms belonging to the framework.

The resulting dependences of the potential energy on the number of ibuprofen molecules inside the pores were in good agreement with the experimental results. In a comparison of the adsorption in potential drug containers such as MOF-74, CD-MOF-1 and bioMOF-100 with the previously studied MIL-53, MIL-100 and MIL-101, assumptions were made about the most probable drug release mechanisms for frameworks that have not yet been investigated (Fig. 13 *a*). For example, the pore diameter in CD-MOF-1 or MOF-74 is very close to the corresponding diameter in MIL-53. Therefore, the adsorbate – adsorbent potential energy profiles virtually do not change with increasing drug loading; hence, the release should be similar to that for MIL-53 and should be slow and require a long period of time. This is due to the presence of polar groups and open metal units in the structures.

In the case of bioMOF-100, which has relatively large mesopores, the interactions between the adsorbent and the adsorbate is expected to be much weaker than in the previous cases and to rapidly decrease with increasing number of adsorbed ibuprofen molecules. The adsorbate – adsorbate contribution to the energy increases linearly with increasing drug loading (Fig. 13 *b*). The bioMOF-100 container was proposed as having the highest adsorption capacity for ibuprofen among all the studied potential containers and

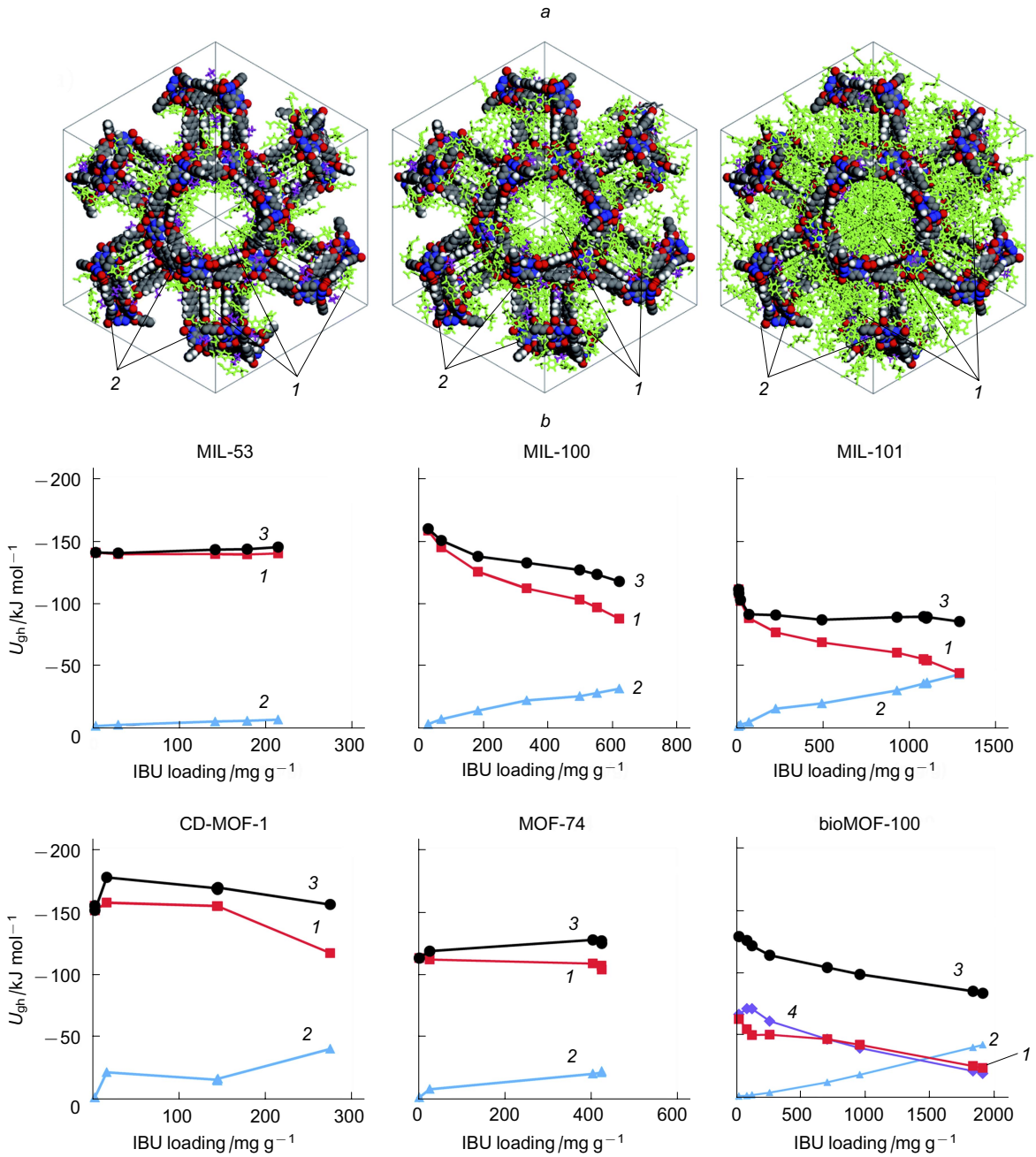


Figure 13. Illustrations of the system behaviour at different ibuprofen loadings into bioMOF-100 (*a*): 329 mg g^{-1} (on the left), 1095 mg g^{-1} (in the middle) and 1975 mg g^{-1} (on the right). (*1*) ibuprofen molecules, (2) DMA cations. Potential energy (U_{gh}) of ibuprofen *vs.* loading in a series of MOFs (*b*).[197]
(*1*) Contribution of the adsorbate – adsorbent interaction to ibuprofen U_{gh}, (*2*) contribution of the adsorbate – adsorbate interaction, (*3*) overall U_{gh}, (*4*) contribution of the DMA – ibuprofen interaction in bioMOF-100.

providing slow kinetically controlled release comparable with that for MIL-101-based systems.

A similar study of Erucar and Keskin[201] describes sorption and retention of bioactive molecules by 24 sorts of MOFs, including the most popular framework-based drug delivery containers and bioMOFs such as MOF-74 and MIL families (Fig. 14). The chosen adsorbates were ibuprofen, caffeine and urea. Computer simulation was accomplished using the configurational bias Monte Carlo algorithm. The interactions of ibuprofen, caffeine and urea with MOFs were modelled using the Lennard-Jones potential and electrostatic potential. The Lennard-Jones parameters for both MOFs and guest molecules were derived from the universal force field (UFF). The method showed good agreement between the data on ibuprofen sorption by the MOF-74, CD-MOF-1, MIL-53(Fe), MIL-100(Fe) and MIL-101(Cr) frameworks. In the case of caffeine and urea, good correlation with the experimental data was also noted. After that,

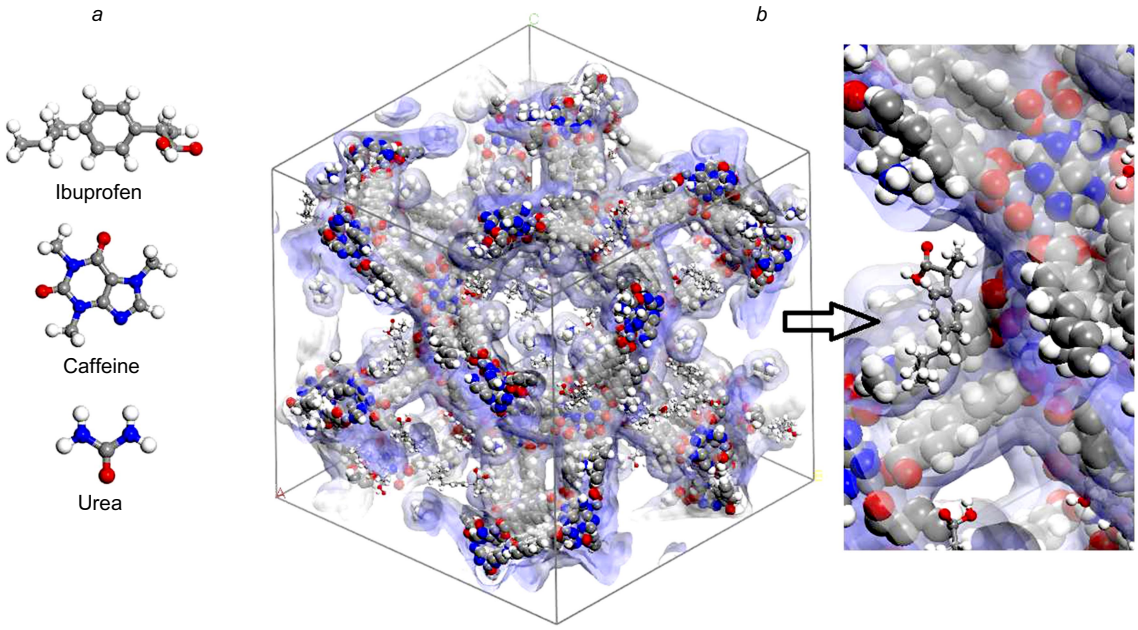


Figure 14. Schematic of the adsorption of drug and cosmetic molecules (*a*) by biocompatible MOFs for ibuprofen (*b*).[201]

the frameworks promising for ibuprofen, caffeine and urea storage and delivery were identified; among these, special mention should be made of the MOF-74 family, which shows good results for ibuprofen sorption. The effect of structure characteristics such as pore volume and diameter on the sorption parameters was also studied for these frameworks.

Liu *et al.*[202] applied the Monte Carlo method to the grand canonical ensemble in order to study the behaviour of the antitumour drug 5-fluorouracil towards sorption in the $\{[Zn_2(fer)_2]\}_n$ frameworks known also as phytochemical MOFs (phytoMOFs). The paper also presents a calculation of the heat of adsorption.

The same drug is mentioned in a publication considering its sorption, as well sorption of hydroxyurea and mercaptopurine molecules, in the zeolite-like imidazolate frameworks, ZIF-7, ZIF-8 and ZIF-9.[203] The calculations were performed using model parameters similar to those used in the previous work.[196] According to computations, despite their moderate pore volume and surface area, these ZIFs show higher sorption capacity towards the considered drugs than other MOFs used for the storage of therapeutic and cosmetic molecules.

The Monte Carlo method can give an idea of not only sorption, but also desorption processes. For example, Kotzabasaki *et al.*,[174] who studied the interaction of the antitumour drug gemcitabine with IRMOF-16 and its functionalized analogue, also carried out predictive calculations on drug desorption. For estimating the relative rate of the release of guest molecules from these frameworks, the researchers carried out Monte Carlo simulations using fully drug-loaded MOFs. New series of simulations were conducted at pressures sufficiently low for all gemcitabine molecules to be desorbed. Then the release process was described as the time dependence of the number of molecules released from the framework. As can be seen from Fig. 15, the drug release is slower in the case of the OH-functionalized IRMOF-16, which almost doubles the time required for complete release.

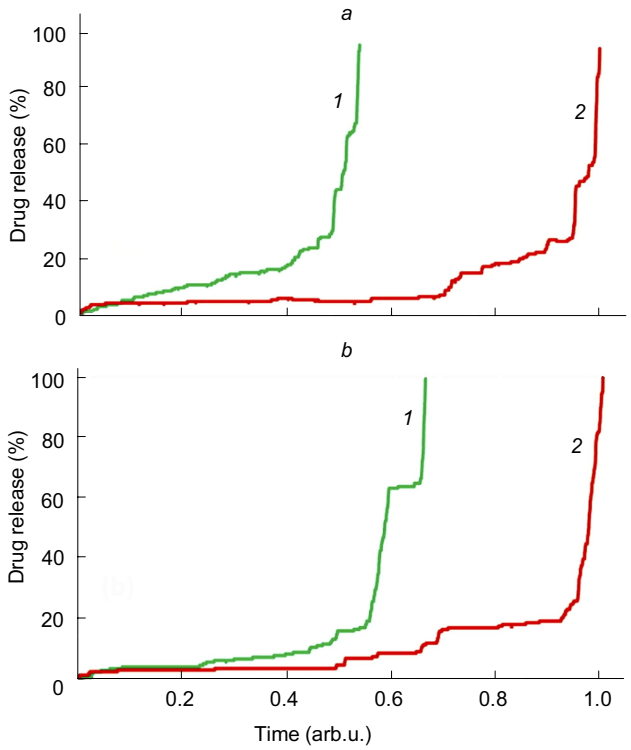


Figure 15. Drug release profiles *vs.* time in a numerical Monte Carlo experiment for IRMOF-16 (*1*) and OH-IRMOF-16 (*2*) at 10^{-8} (*a*) and 10^{-9} Pa (*b*).[174]

Despite the high popularity of the Monte Carlo method for the simulation of framework materials and especially

simulation of the use of MOFs in the medicinal chemistry, the efficiency of this method is still limited by numerous drawbacks that need to be resolved. For example, it is obvious that the accuracy of Monte Carlo calculations directly depends on the extent to which this method is suitable for the given system.

The modern force fields sometimes provide accuracy for specific systems exceeding that of the DFT methods,[203] while being suitable for simulating large-scale systems and lengthy processes, which is especially important for diffusion and adsorption.[204] Nevertheless, adequate simulation of processes of this type requires high-quality force field parameterization (selection of interatomic potentials and calculation of sufficiently accurate parameters for them), which may imply long-lasting systematic work. Currently, there are several classic force fields used to model the sorption processes in MOFs, namely, UFF, Dreiding [205] and Amber [206] (in the order of decreasing frequency of use). In addition, much attention is paid to the development of new force fields designed to model specifically framework materials.

Recently, various force fields have been evaluated in the calculations of the bulk elastic moduli and linear coefficients of thermal expansion for various MOFs. The testing and comparison were performed for the classic force fields (UFF, Dreiding) and for the force fields tailored for application to MOFs (UFF4MOF,[144] BTW-FF [207] and DWES [208]). The results unexpectedly showed that each force field gives adequate values for the parameters and reasonably good description of properties. However, noticeable deviations can be observed for properties depending on the vibrational modes of the framework.[209]

3.2.3. Molecular dynamics

One more highly important method for the simulation of MOF-based drug delivery systems is molecular dynamics. According to this method, the trajectory of each particular atom in the system is determined by integration of the Newtonian mechanics equations of motion. In the classic molecular dynamics, a system is considered to be composed of point atoms with forces acting between them, which are expressed *via* effective potentials.[210]

The main goal of computer simulation of drug delivery systems is to obtain characteristics of the drug release from the framework cavities. Drug release is a dynamic process; hence, for a realistic simulation of the operation of a drug delivery system in a biological medium, it is necessary to estimate the mobility of both guest molecules and MOFs. The most widely used scheme for the establishment of the relationship between the release time and molecular diffusion parameters includes determination of the diffusion coefficients by calculation of the mean square displacement (MSD):

$$\mathrm{MSD}(t) = \frac{1}{N}\sum_{i=1}^{N}\langle|r_i(t) - r_i(0)|^2\rangle \qquad (3)$$

where N is the number of sorbed molecules, $r_i(t)$ is the position of i-th molecule at time t.

For example, in a study of the interaction between gemcitabine and IRMOF-74 systems,[211] the calculation of diffusion coefficients demonstrated that, despite virtually equal pore volumes of IRMOF-74-III and OH-IRMOF-74-III, the mobility of a drug inside IRMOF-74-III is lower. This is attributable to the fact that the CH_3 group in the

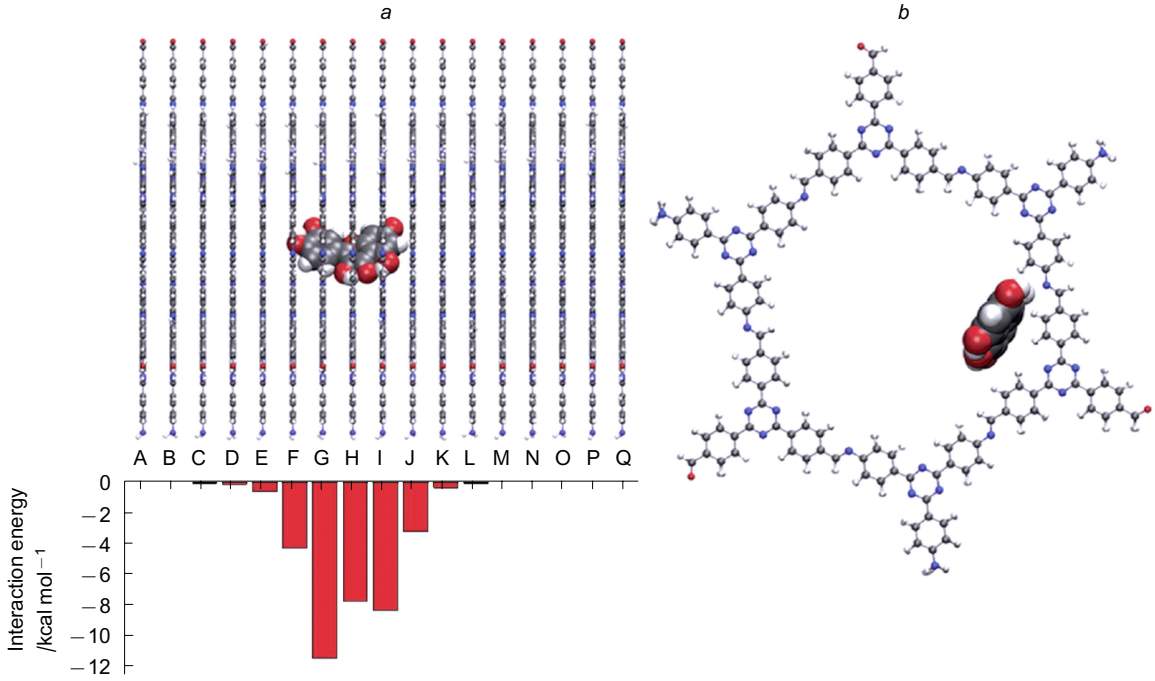


Figure 16. Interaction of quercetin with TTI-COF.[183] Interaction energy between the quercetin molecule and model hexagonal layers (A – Q) (side view) (*a*); snteraction between the quercetin molecule and model pore wall of TTI-COF (top view) (*b*).

IRMOF- 74-III framework occupies a larger effective volume than the hydroxy group in OH-IRMOF-74-III. The same increase in the diffusion mobility with decreasing size of the functional group was observed for glucose adsorption in MIL-101-NH_2 and MIL-101-CH_3.[176]

For description of the molecular mobility and adsorption, molecular dynamics is often supplemented by some other method. Banarao and Jiang [180] determined the lowest energy configurations of ibuprofen in the cavities of Cr-MIL-101 and UMCM-1 by simulated annealing with gradual temperature decrease from 500 to 50 K. Subsequently, the geometry of the identified configurations was optimized by DFT (see Table 7). This confirmed that the strongest binding site in the MIL-101 structure is located in the vicinity of the metal site. Moreover, according to the DFT geometry optimization for the identified configurations performed using the B3LYP functional, the bond length between the oxygen atom of the ibuprofen carboxyl group and the chromium atom of MOF is 2.141 Å, which indicates that the bond of the metal atom with a water molecule has cleaved and, instead, ibuprofen has been coordinated as a ligand. The binding energy between Cr-MIL-101 and ibuprofen is rather high, being equal to -73 kJ mol^{-1}, whereas the geometry optimization of the sorption complex of ibuprofen with UMCM-1 showed the presence of only weak interaction (-35 kJ mol^{-1}).

Regarding the use of covalent organic frameworks (COFs) as delivery systems, the only known to us study in which COFs are considered as potential drug containers at both practical and theoretical levels is the recent investigation of the non-covalent binding of quercetin in the triazine COF pores.[183] The study was based on the molecular dynamics method with the Amber force field. By studying sorption of the single molecule, the most probable sorption trajectory of the molecule in the framework pore was simulated. The geometry optimization was carried out for the quercetin molecule and model COF with hexagonal channels, and the binding energy was -151 kJ mol^{-1} (Fig. 16).

Three different initial orientations of quercetin relative to the 2D framework plane give rise to one and the same structure of the adsorption complex, in which quercetin molecules are arranged perpendicular to the model pore walls. Apart from the C–H π-interactions between the framework hydrogen atoms and the aromatic ring of quercetin, this configuration is also stabilized by interaction between the hydroxyl hydrogen atoms of quercetin and the imine nitrogen atoms of the pore. As the drug molecule moves from one layer to another, the energy loss is significant, which accounts for high mobility of the molecule on the surface.

3.2.4. Molecular docking

Molecular docking, which is traditionally used to simulate the binding of proteins to drug molecules or to other proteins,[212, 213] was proposed for studying the adsorption of drugs in MOF pores.[183] This method is based on the search for new conformations of the molecule being bound and estimation of the change in the binding energy upon change in the positions of model system elements. The binding energy was calculated by the following formula:

$$\Delta G = \left(V_{\text{bound}}^{\text{drug–drug}} - V_{\text{unbound}}^{\text{drug–drug}}\right) + \left(V_{\text{bound}}^{\text{MOF–MOF}} - V_{\text{unbound}}^{\text{MOF–MOF}}\right) + \left(V_{\text{bound}}^{\text{drug–MOF}} - V_{\text{unbound}}^{\text{drug–MOF}} + T\Delta S_{\text{conf}}\right) \quad (4)$$

where ΔG is the Gibbs energy of the system; $V_{\text{bound}}^{\text{drug–drug}}$, $V_{\text{unbound}}^{\text{drug–drug}}$ are the terms describing the interactions of the drug molecule in the bound and unbound states; $V_{\text{bound}}^{\text{MOF–MOF}}$, $V_{\text{unbound}}^{\text{MOF–MOF}}$ are the terms describing the intermolecular interactions in the frameworks in the bound and unbound states; $V_{\text{bound}}^{\text{drug–MOF}}$, $V_{\text{unbound}}^{\text{drug–MOF}}$ are the terms describing the framework–drug interactions in the bound and unbound states; ΔS_{conf} is the term describing the loss of conformational entropy upon binding.[214]

In this case, the contributions of van der Waals forces, electrostatic forces, hydrogen bonds and solvation to the interaction energy can be represented as an equation containing weight factors (W) meant for evaluation of the empirical free energy on the basis of a set of experimentally characterized protein complexes [139, 215]

$$V = W_{\text{udw}} \sum_{i,j} \left(\frac{A_{ij}}{r_{ij}^{12}} - \frac{B_{ij}}{r_{ij}^{6}}\right) + W_{\text{hbond}} \sum_{i,j} E(t) \left(\frac{C_{ij}}{r_{ij}^{12}} - \frac{D_{ij}}{r_{ij}^{10}}\right) + W_{\text{elec}} \sum_{i,j} \frac{q_i q_j}{\varepsilon(r_{ij}) r_{ij}} + W_{\text{sol}} \sum_{i,j} \left(S_i V_j + S_j V_i\right) \exp\left(-r_{ij}^2/2\sigma^2\right) \quad (5)$$

where W_{udw} is the weighing factor responsible for van der Waals interactions; r_{ij} is the distance between the centres of the i-th and j-th species; A_{ij} and B_{ij} are the Lennard-Jones parameters;[204] W_{hbond} is the weighing factor responsible for hydrogen bonds in the system; $E(t)$ is the parameter describing the direction of the hydrogen bond (depends on the angle t of deviation from the ideal binding geometry); C_{ij} and D_{ij} are force field (*e.g.*, Amber force field) parameters;[204] W_{elec} is the weighing factor responsible for the electrostatic interactions in the system; q_i and q_j are charges on the i-th and j-th species; ε is the dielectric permittivity of the medium; W_{sol} is the weighing factor of solvation; S_i and S_j are solvation parameters; V_i and V_j are the volumes occupied by the i-th and j-th species; and σ is the charge density. The first term of the equation is the Lennard-Jones potential for the attraction–repulsion van der Waals forces. The second term corresponds to directed hydrogen bonds based on the 10/12 potential. The third term of the equation reflects the electrostatic interactions approximated by the shielded Coulomb potential. The last term approximates the solvation energy, which depends on the atoms that surround the chosen atom.

For example, docking has been carried out for $[Zn(BDC)(H_2O)_2]_n$ with four biologically active molecules: ibuprofen, amoxicillin, gentamicin and methylene blue.[216] After docking of the guest molecules to the MOF, the lowest energy conformer was chosen for each of the test compounds. The effect of pH on the binding of guest molecules was also estimated *via* docking of drug molecules in the charged state (protonated and deprotonated forms). Ibuprofen binds along one of the sides of the V-shaped groove in the $[Zn(BDC)(H_2O)_2]_n$ surface *via* electrostatic and π–π

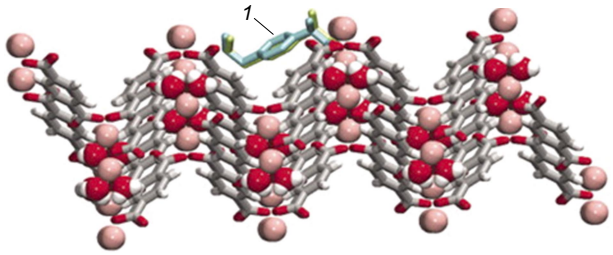


Figure 17. Structure of ibuprofen (*1*) complex with $[Zn(BDC)(H_2O)_2]_n$ based on molecular docking results.[216]

interactions, being arranged along a wall (Fig. 17). Amoxicillin does not completely fit into the V-shaped groove due to steric restrictions. Gentamicin molecule does not bind to $[Zn(BDC)(H_2O)_2]_n$, according to the results of simulation, due to strong electrostatic repulsion.

Yet another example illustrating the applicability of docking simulation to description of the properties of framework material-based drug delivery systems is a study dealing with the morphology and intermolecular interactions in the lansoprazole delivery system with a cyclodextrin-based MOF container (CD-MOF).[87] The docking simulation has shown that drug molecules are preferably collected in cyclodextrin cavities, whereas large hydrophilic pores of CD-MOF are unsuitable for their accommodation. The most favourable location of the molecules is between two cyclodextrin rings.

Thus, the molecular docking procedure provides understanding of the sorption mechanisms and structures of sorption complexes in framework material-based drug delivery systems. For example, the docking results can be used to perform screening of therapeutic agents, *i.e.*, to identify those TAs that are sorbed by the container and those that are not sorbed and must be sorted out. This method makes it possible to identify the most energetically favourable conformation for TA binding and to characterize the binding affinity.

4. Conclusion

At present, the development of novel materials aims to obtain materials that would ensure comprehensive and efficient solution of the priority task. In particular, this refers to the pharmaceutical industry. Active pharmaceutical ingredients are meant for fighting pathogens, but many therapeutic agents have considerable drawbacks, in particular, cytotoxicity and low selectivity. For example, most of anticancer agents exhibit toxicity towards not only damaged cells, but also normal cells. In addition, because of low drug bioavailability, it is often necessary to increase doses, or the conventional dosage form proves to be inconvenient for application.

This problem can be solved by development of drug delivery systems, the main advantage of which would be the absence of targeted change of the drug molecule, with the container material being sensitive to the conditions *in vivo*.

As follows from the survey given here, metal-organic frameworks are ideal candidate materials for this function. High porosity of framework materials allows drug loading to be performed with a high specific weight, which can be controlled by generation of additional sites for noncovalent interactions, with the chemical structure of the active ingredient remaining unchanged. Most of framework materials have hydrophobic inner pores, which makes it possible to improve the pharmacokinetic properties of poorly soluble TAs. The frameworks are characterized by sufficient kinetic and thermodynamic stability for avoiding the burst effect (too fast drug release).

The block structure of MOFs makes it possible to design rationally biocompatible materials and to control the functionalization and morphology of the obtained particles. At the same time, the adjustable configuration of the frameworks has boosted the development and has served as the driving force for promoting computer simulation to the search and exploration of novel materials. Owing to the cluster structure of framework materials, which are composed of organic or organic-inorganic blocks, computer simulation of various physicochemical processes can be carried out at different levels of theory, which, in turn, enables construction of computer models for virtually any stage of drug manufacture.

Nevertheless, computer simulation of the operation of framework materials as drug delivery containers has been started quite recently and the number of publications on this topic is moderate. First of all, this is due to the fact that the design of drug delivery systems based on framework materials is a new and rapidly progressing area. Despite the existence of numerous publications on the simulation of physicochemical processes in framework materials, the application of computational methods to study the properties of MOFs for biomedical applications has a number of limitations. It is also noteworthy that simulation of functioning of biological systems is a resource-intensive and complicated process demanding efforts of specialists in various areas to perform high-quality predictive investigation. Therefore, researchers are faced with the global challenge of combining the experience accumulated in the field of medicinal chemistry, materials science and computational chemistry for the rational design of novel targeted drug delivery systems based on framework materials.

This work was carried out with the financial support of the Ministry of Education and Science of the Russian Federation (Project No. 11.1706.2017/4.6) and the Government of the Russian Federation (Project No. 08-08; A.V.Vinogradov).

Figures 4, 7, 11 and 14 are courtesy of the American Chemical Society; Figures 5, 8 and 13 are courtesy of the Royal Society of Chemistry; Figures 12 and 15 are courtesy of Elsevier; and Figures 16 and 17 are courtesy of John Wiley and Sons.

References

1. J.Čejka. *Angew. Chem., Int. Ed.*, **51**, 4782 (2012)
2. S.Horike, S.Shimomura, S.Kitagawa. *Nat. Chem.*, **1**, 695 (2009)
3. L.Ma, S.Wang, X.Feng, B.Wang. *Chin. Chem. Lett.*, **27**, 1383 (2016)
4. Y.-B.Huang, J.Liang, X.-S.Wang, R.Cao. *Chem. Soc. Rev.*, **46**, 126 (2017)

5. S.R.Batten, N.R.Champness, X.-M.Chen, J.Garcia-Martinez, S.Kitagawa, L.Öhrström, M.O'Keeffe, M.Paik Suh, J.Reedijk. *CrystEngComm*., **14**, 3001 (2012)
6. V.V.Butova, M.A.Soldatov, A.A.Guda, K.A.Lomachenko, C.Lamberti. *Russ. Chem. Rev*., **85**, 280 (2016)
7. R.C.Huxford, J.Della Rocca, W.Lin. *Curr. Opin. Chem. Biol*., **14**, 262 (2010)
8. P.Horcajada, C.Serre, G.Maurin, N.A.Ramsahye, F.Balas, M.Vallet-Regí, M.Sebban, F.Taulelle, G.Férey. *J. Am. Chem. Soc*., **130**, 6774 (2008)
9. C.He, K.Lu, D.Liu, W.Lin. *J. Am. Chem. Soc*., **136**, 5181 (2014)
10. C.He, D.Liu, W.Lin. *Chem. Rev*., **115**, 11079 (2015)
11. H.A.Patel, T.Islamoglu, Z.Liu, S.K.M.Nalluri, A.Samanta, O.Anamimoghadam, C.D.Malliakas, O.K.Farha, J.F.Stoddart. *J. Am. Chem. Soc*., **139**, 11020 (2017)
12. M.Vallet-Regí, F.Balas, D.Arcos. *Angew. Chem., Int. Ed*., **46**, 7548 (2007)
13. J.Della Rocca, D.Liu, W.Lin. *Acc. Chem. Res*., **44**, 957 (2011)
14. M.O'Keeffe, O.M.Yaghi. *Chem. Rev*., **112**, 675 (2012)
15. M.D.Allendorf, V.Stavila. *CrystEngComm*, **17**, 229 (2015)
16. J.J.Perry IV, P.L.Feng, S.T.Meek, K.Leong, F.P.Doty, M.D.Allendorf. *J. Mater. Chem*., **22**, 10235 (2012)
17. E.Sharmin, F.Zafar. In *Metal-Organic Frameworks*. InTech, Rijeka, Croatia, 2016. P. 3
18. S.Kitagawa, M.Kondo. *Bull. Chem. Soc. Jpn*., **71**, 1739 (1998)
19. S.Kitagawa, K.Uemura. *Chem. Soc. Rev*., **34**, 109 (2005)
20. T.Simon-Yarza, S.Rojas, P.Horcajada, C.Serre, in *Comprehensive Biomaterials II*. (Eds K.Healy, D.W.Hutmacher, D.W.Grainger, C.J.Kirkpatrick). (New York: Elsevier, 2017). P. 719
21. P.Horcajada, C.Serre, M.Vallet-Regí, M.Sebban, F.Taulelle, G.Férey. *Angew. Chem., Int. Ed*., **45**, 5974 (2006)
22. J.Zhuang, C.-H.Kuo, L.-Y.Chou, D.-Y.Liu, E.Weerapana, C.-K.Tsung. *ACS Nano*, **8**, 2812 (2014)
23. S.Keskin, S.Kızılel. *Ind. Eng. Chem. Res*., **50**, 1799 (2011)
24. C.Baerlocher, in *Atlas of Zeolite Framework Types*. (Eds C.Baerlocher, L.B.McCusker, D.H.Olson). (New York: Elsevier, 2007). P. 404
25. H.-X.Zhao, Q.Zou, S.-K.Sun, C.Yu, X.Zhang, R.-J.Li, Y.-Y.Fu. *Chem. Sci*., **7**, 5294 (2016)
26. Patent US 9114348 (2013)
27. K.Leus, T.Bogaerts, J.De Decker, H.Depauw, K.Hendrickx, H.Vrielinck, V.Van Speybroeck, P.Van Der Voort. *Microporous Mesoporous Mater*., **226**, 110 (2016)
28. N.Zhang, Y.Yin, S.-J.Xu, W.-S.Chen. *Molecules*, **13**, 1551 (2008)
29. J.L.Arias, M.A.Ruiz, M.López-Viota, Á.V.Delgado. *Colloids Surf., B: Biointerfaces*, **62**, 64 (2008)
30. J.L.Arias, M.López-Viota, Á.V.Delgado, M.A.Ruiz. *Colloids Surf., B: Biointerfaces*, **77**, 111 (2010)
31. G.Takemura, H.Fujiwara. *Prog. Cardiovasc. Dis*., **49**, 330 (2007)
32. X.Gao, M.Zhai, W.Guan, J.Liu, Z.Liu, A.Damirin. *ACS Appl. Mater. Interfaces*, **9**, 3455 (2017)
33. B.Yang, M.Shen, J.Liu, F.Ren. *Pharm. Res*., **34**, 2440 (2017)
34. A.Ma, Z.Luo, C.Gu, B.Li, J.Liu. *Inorg. Chem. Commun*., **77**, 68 (2017)
35. E.H.Zhou, R.Wang, J.Wu, S.W.Qiu, J.Q.Liu, H.R.Zhong, H.D.Zeng, J.W.Xu, J.C.Jin. *Bull. Chem. Soc. Ethiop*., **31**, 457 (2017)
36. E.A.K.Nevethaa, S.Dhanavel, V.Narayanan, A.Stephen. *Int. J. Biol. Macromol*., **95**, 862 (2017)
37. R.Han, Y.Sun, C.Kang, H.Sun, W.Wei. *J. Drug Target*., **25**, 140 (2017)
38. S.Egodawatte, S.Dominguez, S.C.Larsen. *Microporous Mesoporous Mater*., **237**, 108 (2017)
39. B.Kumar, S.Kulanthaivel, A.Mondal, S.Mishra, B.Banerjee, A.Bhaumik, I.Banerjee, S.Giri. *Colloids Surf., B: Biointerfaces*, **150**, 352 (2017)
40. S.Kaur, N.K.Mehra, K.Jain, N.K.Jain. *Artif. Cells, Nanomed., Biotechnol*., **45**, 242 (2017)
41. I.B.Bwatanglang, F.Mohammad, N.A.Yusof, J.Abdullah, N.B.Alitheen, M.Z.Hussein, N.Abu, N.E.Mohammed, N.Nordin, N.R.Zamberi, S.K.Yeap. *J. Colloid Interface Sci*., **480**, 146 (2016)
42. S.Sharma, K.Sethi, I.Roy. *New J. Chem*., **41**, 11860 (2017)
43. F.Shu, D.Lv, X.-L.Song, B.Huang, C.Wang, Y.Yu, S.-C.Zhao. *RSC Adv*., **8**, 6581 (2018)
44. W.Zhou, L.Wang, F.Li, W.Zhang, W.Huang, F.Huo, H.Xu. *Adv. Funct. Mater*., **27**, 1605465 (2017)
45. H.Zhang, W.Jiang, R.Liu, J.Zhang, D.Zhang, Z.Li, Y.Luan. *ACS Appl. Mater. Interfaces*, **9**, 19687 (2017)
46. Z.Zou, S.Li, D.He, X.He, K.Wang, L.Li, X.Yang, H.Li. *J. Mater. Chem. B*, **5**, 2126 (2017)
47. S.Sene, M.T.Marcos-Almaraz, N.Menguy, J.Scola, J.Volatron, R.Rouland, J.-M.Grenèche, S.Miraux, C.Menet, N.Guillou, F.Gazeau, C.Serre, P.Horcajada, N.Steunou. *Chem*, **3**, 303 (2017)
48. A.Bhattacharjee, S.Gumma, M.K.Purkait. *Microporous Mesoporous Mater*., **259**, 203 (2018)
49. S.Li, K.Bi, L.Xiao, X.Shi. *Nanotechnology*, **28**, 495601 (2017)
50. G.V.Khutale, A.Casey. *Eur. J. Pharm. Biopharm*., **119**, 372 (2017)
51. X.Cai, Y.Luo, W.Zhang, D.Du, Y.Lin. *ACS Appl. Mater. Interfaces*, **8**, 22442 (2016)
52. B.Tian, S.Liu, S.Wu, W.Lu, D.Wang, L.Jin, B.Hu, K.Li, Z.Wang, Z.Quan. *Colloids Surf., B: Biointerfaces*, **154**, 287 (2017)
53. S.A.Krovi, E.P.Swindell, T.V.O'Halloran, S.T.Nguyen. *J. Mater. Chem*., **22**, 25463 (2012)
54. I.Imaz, M.Rubio-Martínez, J.An, I.Solé-Font, N.L.Rosi, D.Maspoch. *Chem. Commun*., **47**, 7287 (2011)
55. S.Rojas, T.Devic, P.Horcajada. *J. Mater. Chem. B*, **5**, 2560 (2017)
56. S.L.Anderson, K.C.Stylianou. *Coord. Chem. Rev*., **349**, 102 (2017)
57. J.Zhuang, A.P.Young, C.K.Tsung. *Small*, **13**, 1700880 (2017)

58. H.Cai, M.Li, X.-R.Lin, W.Chen, G.-H.Chen, X.-C.Huang, D.Li. *Angew. Chem., Int. Ed.*, **54**, 10454 (2015)
59. H.Cai, L.-L.Xu, H.-Y.Lai, J.-Y.Liu, S.W.Ng, D.Li. *Chem. Commun.*, **53**, 7917 (2017)
60. D.Feng, T.-F.Liu, J.Su, M.Bosch, Z.Wei, W.Wan, D.Yuan, Y.-P.Chen, X.Wang, K.Wang, X.Lian, Z.-Y.Gu, J.Park, X.Zou, H.-C.Zhou. *Nat. Commun.*, **6**, 5979 (2015)
61. Y.-P.He, N.Zhou, Y.-X.Tan, F.Wang, J.Zhang. *J. Solid State Chem.*, **238**, 241 (2016)
62. M.-Y.Li, F.Wang, Z.-G.Gu, J.Zhang. *RSC Adv.*, **7**, 4872 (2017)
63. E.A.K.Nivethaa, S.Dhanavel, V.Narayanan, A.Stephen. *Inorg. Chem. Commun.*, **95**, 68 (2017)
64. P.A.Sontz, J.B.Bailey, S.Ahn, F.A.Tezcan. *J. Am. Chem. Soc.*, **137**, 11598 (2015)
65. D.Fujita, M.Fujita. *ACS Cent. Sci.*, **1**, 352 (2015)
66. M.Hou, H.Zhao, Y.Feng, J.Ge. *Bioresour. Bioprocess.*, **4**, 40 (2017)
67. D.J.Levine, T.Runčevski, M.T.Kapelewski, B.K.Keitz, J.Oktawiec, D.A.Reed, J.A.Mason, H.Z.H.Jiang, K.A.Colwell, C.M.Legendre, S.A.FitzGerald, J.R.Long. *J. Am. Chem. Soc.*, **138**, 10143 (2016)
68. R.J.Radford, M.Lawrenz, P.C.Nguyen, J.A.McCammon, F.A.Tezcan. *Chem. Commun.*, **47**, 313 (2011)
69. W.-L.Liu, S.-H.Lo, B.Singco, C.-C.Yang, H.-Y.Huang, C.-H.Lin. *J. Mater. Chem. B*, **1**, 928 (2013)
70. L.Wang, C.Gong, Y.Shen, W.Ye, M.Xu, Y.Song. *Sens. Actuators, B: Chem.*, **242**, 625 (2017)
71. J.Mehta, N.Bhardwaj, S.K.Bhardwaj, K.-H.Kim, A.Deep, *Coord. Chem. Rev.*, **322**, 30 (2016)
72. J.An, S.J.Geib, N.L.Rosi. *J. Am. Chem. Soc.*, **131**, 8376 (2009)
73. J.An, O.K.Farha, J.T.Hupp, E.Pohl, J.I.Yeh, N.L.Rosi. *Nat. Commun.*, **3**, 604 (2012)
74. S.R.Miller, D.Heurtaux, T.Baati, P.Horcajada, J.-M.Grenèche, C.Serre. *Chem. Commun.*, **46**, 4526 (2010)
75. S.R.Miller, P.Horcajada, C.Serre. *CrystEngComm*, **13**, 1894 (2011)
76. T.Chalati, P.Horcajada, R.Gref, P.Couvreur, C.Serre. *J. Mater. Chem.*, **21**, 2220 (2011)
77. E.Alvarez, A.G.Marquez, T.Devic, N.Steunou, C.Serre, C.Bonhomme, C.Gervais, I.Izquierdo-Barba, M.Vallet-Regi, D.Laurencin, F.Mauri, P.Horcajada. *CrystEngComm*, **15**, 9899 (2013)
78. C.Tamames-Tabar, E.Imbuluzqueta, N.Guillou, C.Serre, S.R.Miller, E.Elkaïm, P.Horcajada, M.J.Blanco-Prieto. *CrystEngComm*, **17**, 456 (2015)
79. A.D.Burrows, M.Jurcic, L.L.Keenan, R.A.Lane, M.F.Mahon, M.R.Warren, H.Nowell, M.Paradowski, J.Spencer. *Chem. Commun.*, **49**, 11260 (2013)
80. L.Cooper, T.Hidalgo, M.Gorman, T.Lozano-Fernández, R.Simón-Vázquez, C.Olivier, N.Guillou, C.Serre, C.Martineau, F.Taulelle, D.Damasceno-Borges, G.Maurin, Á.González-Fernández, P.Horcajada, T.Devic. *Chem. Commun.*, **51**, 5848 (2015)
81. J.Navarro-Sánchez, A.I.Argente-García, Y.Moliner-Martínez, D.Roca-Sanjuán, D.Antypov, P.Campíns-Falcó, M.J.Rosseinsky, C.Martí-Gastaldo. *J. Am. Chem. Soc.*, **139**, 4294 (2017)
82. J.B.Bailey, L.Zhang, J.A.Chiong, S.Ahn, F.A.Tezcan. *J. Am. Chem. Soc.*, **139**, 8160 (2017)
83. Z.Liu, S.K.M.Nalluri, J.F.Stoddart. *Chem. Soc. Rev.*, **46**, 2459 (2017)
84. B.Liu, H.Li, X.Xu, X.Li, N.Lv, V.Singh, J.F.Stoddart, P.York, X.Xu, R.Gref, J.Zhang. *Int. J. Pharm.*, **514**, 212 (2016)
85. D.Wu, J.J.Gassensmith, D.Gouvêa, S.Ushakov, J.F.Stoddart, A.Navrotsky. *J. Am. Chem. Soc.*, **135**, 6790 (2013)
86. H.Li, N.Lv, X.Li, B.Liu, J.Feng, X.Ren, T.Guo, D.Chen, J.F.Stoddart, R.Gref, J.Zhang. *Nanoscale*, **9**, 7454 (2017)
87. X.Li, T.Guo, L.Lachmanski, F.Manoli, M.Menendez-Miranda, I.Manet, Z.Guo, L.Wu, J.Zhang, R.Gref. *Int. J. Pharm.*, **531**, 424 (2017)
88. K.J.Hartlieb, D.P.Ferris, J.M.Holcroft, I.Kandela, C.L.Stern, M.S.Nassar, Y.Y.Botros, J.F.Stoddart. *Mol. Pharm.*, **14**, 1831 (2017)
89. B.Liu, Y.He, L.Han, V.Singh, Xia.Xu, T.Guo, F.Meng, X.Xu, P.York, Z.Liu, J.Zhang. *Cryst. Growth Des.*, **17**, 1654 (2017)
90. X.Xu, C.Wang, H.Li, X.Li, B.Liu, V.Singh, S.Wang, L.Sun, R.Gref, J.Zhang. *J. Chromatogr., A*, **1488**, 37 (2017)
91. J.Sha, X.Yang, L.Sun, X.Zhang, S.Li, J.Li, N.Sheng. *Polyhedron*, **127**, 396 (2017)
92. H.Lu, X.Yang, S.Li, Y.Zhang, J.Sha, C.Li, J.Sun. *Inorg. Chem. Commun.*, **61**, 48 (2015)
93. N.ul Qadir, S.A.M.Said, H.M.Bahaidarah. *Microporous Mesoporous Mater.*, **201**, 61 (2015)
94. Y.Li, F.Liang, H.Bux, W.Yang, J.Caro. *J. Membr. Sci.*, **354**, 48 (2010)
95. S.Rojas, F.J.Carmona, C.R.Maldonado, E.Barea, J.A.R.Navarro. *New J. Chem.*, **40**, 5690 (2016)
96. D.Raubenheimer, K.P.Lee, S.J.Simpson. *Proc. R. Soc. B: Biological Sci.*, **272**, 2429 (2005)
97. C.-Y.Sun, C.Qin, X.-L.Wang, Z.-M.Su. *Expert Opin. Drug Deliv.*, **10**, 89 (2013)
98. T.Mosmann. *J. Immunol. Methods*, **65**, 55 (2013)
99. *In vitro Toxicity Testing Protocols*. (Eds S.O'Hare, C.K.Atterwill). (Totowa, NJ: Humana Press, 1995)
100. L.V.Anikina, S.A.Pukhov, E.S.Dubrovskaya, S.V.Afanas'eva, S.G.Klochkov. *Fundamental. Issledovaniya*, (12-7), 1423 (2014)
101. M.Hanke, H.K.Arslan, S.Bauer, O.Zybaylo, C.Christophis, H.Gliemann, A.Rosenhahn, C.Wöll. *Langmuir*, **28**, 6877 (2012)
102. F.R.S.Lucena, L.C.C.de Araújo, M.do D.Rodrigues, T.G.da Silva, V.R.A.Pereira, G.C.G.Militão, D.A.F.Fontes, P.J.Rolim-Neto, F.F.da Silva, S.C.Nascimento. *Biomed. Pharmacother.*, **67**, 707 (2013)
103. K.M.L.Taylor-Pashow, J.Della Rocca, Z.Xie, S.Tran, W.Lin. *J. Am. Chem. Soc.*, **131**, 14261 (2009)
104. W.J.Rieter, K.M.Pott, K.M.L.Taylor, W.Lin. *J. Am. Chem. Soc.*, **130**, 11584 (2008)

105. P.Horcajada, T.Chalati, C.Serre, B.Gillet, C.Sebrie, T.Baati, J.F.Eubank, D.Heurtaux, P.Clayette, C.Kreuz, J.-S.Chang, Y.K.Hwang, V.Marsaud, P.-N.Bories, L.Cynober, S.Gil, G.Férey, P.Couvreur, R.Gref. *Nat. Mater.*, **9**, 172 (2009)
106. M.D.Rowe, D.H.Thamm, S.L.Kraft, S.G.Boyes. *Biomacromolecules*, **10**, 983 (2009)
107. D.Wang, J.Zhou, R.Chen, R.Shi, G.Zhao, G.Xia, R.Li, Z.Liu, J.Tian, H.Wang, Z.Guo, H.Wang, Q.Chen. *Biomaterials*, **100**, 27 (2016)
108. A.Ray Chowdhuri, D.Bhattacharya, S.K.Sahu. *Dalton Trans.*, **45**, 2963 (2016)
109. M.A.Chowdhury. *J. Biomed. Mater. Res., Part A*, **105**, 1184 (2017)
110. W.Chen, C.Wu. *Dalton Trans.*, **47**, 2114 (2018)
111. N.A.Mohamed, R.P.Davies, P.D.Lickiss, B.Ahmetaj-Shala, D.M.Reed, H.H.Gashaw, H.Saleem, G.R.Freeman, P.M.George, S.J.Wort, D.Morales-Cano, B.Barreira, T.D.Tetley, A.H.Chester, M.H.Yacoub, N.S.Kirkby, L.Moreno, J.A.Mitchell. *Pulm. Circ.*, **7**, 643 (2017)
112. T.Baati, L.Njim, F.Neffati, A.Kerkeni, M.Bouttemi, R.Gref, M.F.Najjar, A.Zakhama, P.Couvreur, C.Serre, P.Horcajada. *Chem. Sci.*, **4**, 1597 (2013)
113. Y.Zhang, J.Wang. *Inorg. Chim. Acta*, **477**, 8 (2018)
114. T.Kundu, S.Mitra, P.Patra, A.Goswami, D.Díaz, R.Banerjee. *Chem. – Eur. J.*, **20**, 10514 (2014)
115. J.G.Vitillo, C.Atzori, B.Civalleri, N.Barbero, C.Barolo, F.Bonino, in *Hybrid Organic-Inorganic Interfaces: Towards Advanced Functional Materials*. (Eds M.H.Delville, A.Taubert). (Weinheim: Wiley, 2018). P. 978
116. A.C.McKinlay, R.E.Morris, P.Horcajada, G.Férey, R.Gref, P.Couvreur, C.Serre. *Angew. Chem., Int. Ed.*, **49**, 6260 (2010)
117. M.Gaumet, A.Vargas, R.Gurny, F.Delie. *Eur. J. Pharm. Biopharm.*, **69**, 1 (2008)
118. R.Liu, T.Yu, Z.Shi, Z.Wang. *Int. J. Nanomed.*, **11**, 1187 (2016)
119. C.Orellana-Tavra, S.A.Mercado, D.Fairen-Jimenez. *Adv. Health. Mater.*, **5**, 2261 (2016)
120. S.Wang, R.G.Larson. *Langmuir*, **31**, 1262 (2015)
121. P.V.Messina, R.Rial, J.M.Ruso. *Curr. Pharm. Des.*, **22**, 5211 (2016)
122. X.Cheng, J.-K.Kim, Y.Kim, J.U.Bowie, W.Im. *Biochim. Biophys. Acta — Biomembr.*, **1858**, 1566 (2016)
123. M.Meunier, A.Goupil, P.Lienard. *Int. J. Pharm.*, **526**, 157 (2017)
124. A.Accardo, G.Morelli. *Biopolymers*, **104**, 462 (2015)
125. D.Karst, Y.Yang. *J. Biomed. Mater. Res., Part A*, **88**, 255 (2009)
126. N.K.Gayathri, V.Aparna, S.Maya, R.Biswas, R.Jayakumar, C.G.Mohan. *Carbohydr. Polym.*, **177**, 67 (2017)
127. A.J.Makarucha, N.Todorova, I.Yarovsky. *Eur. Biophys. J.*, **40**, 103 (2011)
128. L.Liang, J.W.Shen, Q.Wang. *Colloids Surf., B: Biointerfaces*, **153**, 168 (2017)
129. Z.Ge, Y.Wang. In *Annual Reports in Computational Chemistry. Vol. 12*. (Ed. D.A.Dixon). Elsevier, New York, 2016. P. 159
130. R.Laitinen, P.A.Priemel, S.Surwase, K.Graeser, C.J.Strachan, H.Grohganz, T.Rades in *Amorphous Solid Dispersions*. (Eds N.Shah, H.Sandhu, D.S.Choi, H.Chokshi, A.W.Malick). (New York: Springer, 2014). P. 699
131. Y.-C.Li, S.Rissanen, M.Stepniewski, O.Cramariuc, T.Róg, S.Mirza, H.Xhaard, M.Wytrwal, M.Kepczynski, A.Bunker. *J. Phys. Chem. B*, **116**, 7334 (2012)
132. P.Decuzzi. *ACS Nano*, **10**, 8133 (2016)
133. C.M.Park, K.H.Chu, J.Heo, N.Her, M.Jang, A.Son, Y.Yoon. *J. Hazard. Mater.*, **309**, 133 (2016)
134. T.Panczyk, T.P.Warzocha, P.J.Camp. *J. Phys. Chem. C*, **114**, 21299 (2010)
135. M.Ramezanpour, S.S.W.Leung, K.H.Delgado-Magnero, B.Y.M.Bashe, J.Thewalt, D.P.Tieleman. *Biochim. Biophys. Acta — Biomembr.*, **1858**, 1688 (2016)
136. *Adverse Effects of Engineered Nanomaterials: Exposure, Toxicology, and Impact on Human Health*. (Eds B.Fadeel, A.Pietroiusti, A.A.Shvedova). (New York: Academic Press, 2017)
137. R.Chen, J.E.Riviere. *Wiley Interdiscip. Rev.: Nanomed. Nanobiotechnol.*, **9**, 1440 (2017)
138. G.Sliwoski, S.Kothiwale, J.Meiler, E.W.Lowe. *Pharmacol. Rev.*, **66**, 334 (2014)
139. M.P.Allen. *Comput. Soft Matter*, **23**, 1 (2004)
140. J.Wang, M.Shu, Yuanq Wang, Y.Hu, Yuanl Wang, Y.Luo, Z.Lin. *Mol. BioSyst.*, **12**, 3396 (2016)
141. S.Dhanasekaran. *Int. J. Immunother. Cancer Res.*, **8591**, 1 (2015)
142. M.A.Addicoat, D.E.Coupry, T.Heine. *J. Phys. Chem. A*, **118**, 9607 (2014)
143. A.H.Larsen, J.J.Mortensen, J.Blomqvist, I.E.Castelli, R.Christensen, M.Dułak, J.Friis, M.N.Groves, B.Hammer, C.Hargus, E.D.Hermes, P.C.Jennings, P.B.Jensen, J.Kermode, J.R.Kitchin, E.L.Kolsbjerg, J.Kubal, K.Kaasbjerg, S.Lysgaard, J.B.Maronsson, T.Maxson, T.Olsen, L.Pastewka, A.Peterson, C.Rostgaard, J.Schiøtz, O.Schütt, M.Strange, K.S.Thygesen, T.Vegge, L.Vilhelmsen, M.Walter, Z.Zeng, K.W.Jacobsen. *J. Phys.: Condens. Matter*, **29**, 273002 (2017)
144. D.E.Coupry, M.A.Addicoat, T.Heine. *J. Chem. Theory Comput.*, **12**, 5215 (2016)
145. T.Van Heest, S.L.Teich-McGoldrick, J.A.Greathouse, M.D.Allendorf, D.S.Sholl. *J. Phys. Chem. C*, **116**, 13183 (2012)
146. A.L.Myers, J.M.Prausnitz. *AIChE J.*, **11**, 121 (1965)
147. T.F.Willems, C.H.Rycroft, M.Kazi, J.C.Meza, M.Haranczyk. *Microporous Mesoporous Mater.*, **149**, 134 (2012)
148. Y.G.Chung, J.Camp, M.Haranczyk, B.J.Sikora, W.Bury, V.Krungleviciute, T.Yildirim, O.K.Farha, D.S.Sholl, R.Q.Snurr. *Chem. Mater.*, **26**, 6185 (2014)
149. M.Tong, Y.Lan, Q.Yang, C.Zhong. *Chem. Eng. Sci.*, **168**, 456 (2017)
150. Y.J.Colón, R.Q.Snurr. *Chem. Soc. Rev.*, **43**, 5735 (2014)

151. C.R.Groom, I.J.Bruno, M.P.Lightfoot, S.C.Ward. *Acta Crystallogr., Sect. B: Struct. Sci. Cryst. Eng. Mater.*, **72**, 171 (2016)
152. C.Mellot Draznieks, J.M.Newsam, A.M.Gorman, C.M.Freeman, G.Férey. *Angew. Chem., Int. Ed.*, **39**, 2270 (2000)
153. M.Li, D.Li, M.O'Keeffe, O.M.Yaghi. *Chem. Rev.*, **114**, 1343 (2013)
154. H.Deng, C.J.Doonan, H.Furukawa, R.B.Ferreira, J.Towne, C.B.Knobler, B.Wang, O.M.Yaghi. *Science*, **327**, 846 (2010)
155. F.A.Almeida Paz, J.Klinowski, S.M.F.Vilela, J.P.C.Tomé, J.A.S.Cavaleiro, J.Rocha. *Chem. Soc. Rev.*, **41**, 1088 (2012)
156. F.Trousselet, A.Archereau, A.Boutin, F.-X.Coudert. *J. Phys. Chem. C*, **120**, 24885 (2016)
157. F.-X.Coudert, A.H.Fuchs. *Coord. Chem. Rev.*, **307**, 211 (2016)
158. R.Dovesi, R.Orlando, A.Erba, C.M.Zicovich-Wilson, B.Civalleri, S.Casassa, L.Maschio, M.Ferrabone, M.De La Pierre, P.D'Arco, Y.Noël, M.Causà, M.Rérat, B.Kirtman. *Int. J. Quantum Chem.*, **114**, 1287 (2014)
159. F.J.Devlin, J.W.Finley, P.J.Stephens, M.J.Frisch. *J. Phys. Chem.*, **99**, 16883 (1995)
160. J.P.Perdew, A.Ruzsinszky, G.I.Csonka, O.A.Vydrov, G.E.Scuseria, L.A.Constantin, X.Zhou, K.Burke. *Phys. Rev. Lett.*, **100**, 136406 (2008)
161. S.Grimme. *J. Comput. Chem.*, **27**, 1787 (2006)
162. O.Ivanciuc. *Curr. Comput.-Aided Drug Des.*, **9**, 153 (2013)
163. R.S.Mulliken. *J. Chem. Phys.*, **23**, 1833 (1955)
164. S.M.J.Rogge, A.Bavykina, J.Hajek, H.Garcia, A.I.Olivos-Suarez, A.Sepúlveda-Escribano, A.Vimont, G.Clet, P.Bazin, F.Kapteijn, M.Daturi, E.V.Ramos-Fernandez, F.X.Llabrés i Xamena, V.Van Speybroeck, J.Gascon. *Chem. Soc. Rev.*, **46**, 3134 (2017)
165. E.A.Pidko, E.J.M.Hensen, in *Metal Organic Frameworks as Heterogeneous Catalysts*. (Eds F.X.Llabrés i Xamena, J.Gascon, J.Spivey). (London: Royal Society of Chemistry, 2013). P. 209
166. J.P.Perdew, J.A.Chevary, S.H.Vosko, K.A.Jackson, M.R.Pederson, D.J.Singh, C.Fiolhais. *Phys. Rev. B*, **46**, 6671 (1992)
167. J.P.Perdew, K.Burke, M.Ernzerhof. *Phys. Rev. Lett.*, **77**, 3865 (1996)
168. F.Weigend, R.Ahlrichs. *Phys. Chem. Chem. Phys.*, **7**, 3297 (2005)
169. A.Schäfer, H.Horn, R.Ahlrichs. *J. Chem. Phys.*, **97**, 2571 (1992)
170. R.Ditchfield, W.J.Hehre, J.A.Pople. *J. Chem. Phys.*, **54**, 724 (1971)
171. S.Kossmann, F.Neese. *Chem. Phys. Lett.*, **481**, 240 (2009)
172. S.Foletti, H.Bluhm, D.Mahalu, V.Umansky, A.Yacoby. *Nat. Phys.*, **5**, 903 (2009)
173. Y.Inada, H.Orita. *J. Comput. Chem.*, **29**, 225 (2008)
174. M.Kotzabasaki, E.Tylianakis, E.Klontzas, G.E.Froudakis. *Chem. Phys. Lett.*, **685**, 114 (2017)
175. E.N.Koukaras, A.D.Zdetsis, G.E.Froudakis. *J. Phys. Chem. Lett.*, **2**, 272 (2011)
176. K.M.Gupta, K.Zhang, J.Jiang. *Sci. Rep.*, **5**, 12821 (2015)
177. K.Liu, S.Zhang, X.Hu, K.Zhang, A.Roy, G.Yu. *Environ. Sci. Technol.*, **49**, 8657 (2015)
178. D.Cunha, M.Ben Yahia, S.Hall, S.R.Miller, H.Chevreau, E.Elkaïm, G.Maurin, P.Horcajada, C.Serre. *Chem. Mater.*, **25**, 2767 (2013)
179. T.Chalati, P.Horcajada, P.Couvreur, C.Serre, M.Ben Yahia, G.Maurin, R.Gref. *Nanomedicine*, **6**, 1683 (2011)
180. R.Babarao, J.Jiang. *J. Phys. Chem. C*, **113**, 18287 (2009)
181. B.Supronowicz, A.Mavrandonakis, T.Heine. *J. Phys. Chem. C*, **119**, 3024 (2015)
182. M.Gomar, S.Yeganegi. *Microporous Mesoporous Mater.*, **252**, 167 (2017)
183. V.S.Vyas, M.Vishwakarma, I.Moudrakovski, F.Haase, G.Savasci, C.Ochsenfeld, J.P.Spatz, B.V.Lotsch. *Adv. Mater.*, **28**, 8749 (2016)
184. E.N.Koukaras, T.Montagnon, P.Trikalitis, D.Bikiaris, A.D.Zdetsis, G.E.Froudakis. *J. Phys. Chem. C*, **118**, 8885 (2014)
185. M.Pitoňák, J.Řezáč, P.Hobza. *Phys. Chem. Chem. Phys.*, **12**, 9611 (2010)
186. S.Devautour-Vinot, C.Martineau, S.Diaby, M.Ben-Yahia, S.Miller, C.Serre, P.Horcajada, D.Cunha, F.Taulelle, G.Maurin. *J. Phys. Chem. C*, **117**, 11694 (2013)
187. Q.Chen, Q.-W.Chen, C.Zhuang, P.-P.Tang, N.Lin, L.-Q.Wei. *Inorg. Chem. Commun.*, **79**, 78 (2017)
188. S.Grimme. *J. Comput. Chem.*, **25**, 1463 (2004)
189. J.Černý, P.Hobza. *Phys. Chem. Chem. Phys.*, **7**, 1624 (2005)
190. S.Grimme. *Wiley Interdiscip. Rev. Comput.: Mol. Sci.*, **1**, 211 (2011)
191. O.A.Vydrov, T.Van Voorhis. *J. Chem. Phys.*, **133**, 244103 (2010)
192. M.Dion, H.Rydberg, E.Schröder, D.C.Langreth, B.I.Lundqvist. *Phys. Rev. Lett.*, **92**, 246401 (2004)
193. N.Metropolis, A.W.Rosenbluth, M.N.Rosenbluth, A.H.Teller, E.Teller. *J. Chem. Phys.*, **21**, 1087 (1953)
194. J.I.Siepmann, D.Frenkel. *Mol. Phys.*, **75**, 59 (1992)
195. M.N.Rosenbluth, A.W.Rosenbluth. *J. Chem. Phys.*, **23**, 356 (1955)
196. D.Frenkel, B.Smit, in *Understanding Molecular Simulation: from Algorithms to Applications*. (Eds D.Frenkel, B.Smit). (New York: Elsevier, 2001). P. 111
197. M.C.Bernini, D.Fairen-Jimenez, M.Pasinetti, A.J.Ramirez-Pastor, R.Q.Snurr. *J. Mater. Chem. B*, **2**, 766 (2014)
198. P.D.C.Dietzel, R.Blom, H.Fjellvåg. *Eur. J. Inorg. Chem.*, **2008**, 3624 (2008)
199. R.S.Forgan, R.A.Smaldone, J.J.Gassensmith, H.Furukawa, D.B.Cordes, Q.Li, C.E.Wilmer, Y.Y.Botros, R.Q.Snurr, A.M.Z.Slawin, J.F.Stoddart. *J. Am. Chem. Soc.*, **134**, 406 (2012)
200. A.N.Zhenguo, L.I.Bing, J.Yuan, J.Zhang. *Mater. Rev.*, **3**, 001 (2012)
201. I.Erucar, S.Keskin. *Ind. Eng. Chem. Res.*, **55**, 1929 (2016)
202. J.-Q.Liu, X.-F.Li, C.-Y.Gu, J.C.S.da Silva, A.L.Barros, S.Alves Jr., B.-H.Li, F.Ren, S.R.Batten, T.A.Soares. *Dalton Trans.*, **44**, 19370 (2015)

203. J.Nyman, O.S.Pundyke, G.M.Day. *Phys. Chem. Chem. Phys.*, **18**, 15828 (2016)
204. J.D.Evans, K.E.Jelfs, G.M.Day, C.J.Doonan. *Chem. Soc. Rev.*, **46**, 3286 (2017)
205. S.L.Mayo, B.D.Olafson, W.A.Goddard III. *J. Phys. Chem*, **94**, 8897 (1990)
206. W.D.Cornell, P.Cieplak, C.I.Bayly, I.R.Gould, K.M.Merz, D.M.Ferguson, D.C.Spellmeyer, T.Fox, J.W.Caldwell, P.A.Kollman. *J. Am. Chem. Soc.*, **117**, 5179 (1995)
207. J.K.Bristow, D.Tiana, A.Walsh. *J. Chem. Theory Comput.*, **10**, 4644 (2014)
208. D.Dubbeldam, K.S.Walton, D.E.Ellis, R.Q.Snurr. *Angew. Chem., Int. Ed.*, **46**, 4496 (2007)
209. P.G.Boyd, S.M.Moosavi, M.Witman, B.Smit. *J. Phys. Chem. Lett.*, **8**, 357 (2017)
210. F.Jensen, in *Introduction to Computational Chemistry*. (Ed. F.Jensen). (Hoboken, NJ: Wiley, 2017). P. 600
211. M.Kotzabasaki, I.Galdadas, E.Tylianakis, E.Klontzas, Z.Cournia, G.E.Froudakis. *J. Mater. Chem. B*, **5**, 3277 (2017)
212. G.M.Morris, D.S.Goodsell, R.S.Halliday, R.Huey, W.E.Hart, R.K.Belew, A.J.Olson. *J. Comput. Chem.*, **19**, 1639 (1998)
213. R.D.Taylor, P.J.Jewsbury, J.W.Essex. *J. Comput.-Aided. Mol. Des.*, **16**, 151 (2002)
214. G.R.Smith, M.J.E.Sternberg. *Curr. Opin. Struct. Biol.*, **12**, 28 (2002)
215. R.Huey, G.M.Morris, A.J.Olson, D.S.Goodsell. *J. Comput. Chem.*, **28**, 1145 (2007)
216. M.O.Rodrigues, M.V.de Paula, K.A.Wanderley, I.B.Vasconcelos, S.Alves, T.A.Soares. *Int. J. Quantum Chem.*, **112**, 3346 (2012)